

# 4 The Physics of Doped Mott Insulators

Robert Eder

Karlsruhe Institute of Technology

Institute for Quantum Materials and Technologies

## Contents

<b>1</b>	<b>Introduction</b>	<b>2</b>
<b>2</b>	<b>The basic concept: Hubbard-I approximation</b>	<b>3</b>
<b>3</b>	<b>Antiferromagnets</b>	<b>8</b>
3.1	Spin exchange . . . . .	8
3.2	Magnons in an antiferromagnet . . . . .	9
3.3	One hole in an antiferromagnet . . . . .	12
<b>4</b>	<b>Spin liquids</b>	<b>18</b>
4.1	Dimer basis . . . . .	18
4.2	Spin excitations . . . . .	21
4.3	Doped holes . . . . .	25
<b>5</b>	<b>Summary and Outlook</b>	<b>28</b>

# 1 Introduction

Following the discovery of copper oxide superconductors with their spectacularly high superconducting transition temperatures by Bednorz and Müller [1], the problem of the doped Mott insulator has become a central issue in solid state physics. Still, after more than 30 years of research and thousands of papers devoted to this subject, there is no generally accepted theory for this problem. So what exactly do we mean by ‘doped Mott insulator’ and why is this problem so hard to solve?

Let us consider a two-dimensional square lattice with lattice constant  $a = 1$ , which consists of  $N = L^2$  sites and impose periodic boundary conditions with period  $L$  along both the  $x$ - and  $y$ -direction. We denote the number of electrons with spin  $\sigma$  by  $N_\sigma$ , the total number of electrons by  $N_e = N_\uparrow + N_\downarrow$ . Also, we denote densities per site by  $n$ , for example  $n_e = N_e/N$ . To explain the idea of a Mott-insulator it would be neither necessary that the system is two-dimensional, nor that we have a square lattice, but this is the suitable geometry to describe the  $\text{CuO}_2$  planes in copper oxide superconductors. We assume that there is one  $s$ -like atomic orbital  $|\phi_i\rangle$  centered at each lattice site  $i$ . Orbitals on different sites are assumed to be orthogonal,  $\langle\phi_i|\phi_j\rangle = \delta_{i,j}$ , but there may be nonvanishing matrix elements of the Hamiltonian – that means the kinetic and potential energy – between them,  $\langle\phi_i|H|\phi_j\rangle = -t_{i,j}$ . We assume that the orbital  $|\phi\rangle$  is the same for each lattice site, whence the matrix element  $\langle\phi_i|\phi_j\rangle$  depends only on the distance between  $i$  and  $j$ ,  $t_{i,j} = t_{\mathbf{R}_i - \mathbf{R}_j}$ . We also assume that the atomic orbital  $|\phi_i\rangle$  decays exponentially,  $\langle\mathbf{r}|\phi_i\rangle \propto e^{-|\mathbf{r} - \mathbf{R}_i|/\zeta}$ , so we expect  $t_{\mathbf{R}} \propto e^{-|\mathbf{R}|/\zeta}$  and  $t_{i,j}$  will differ appreciably from zero only for close neighbors. Introducing operators  $c_{i,\sigma}^\dagger$  which create an electron of  $z$ -spin  $\sigma$  in the orbital  $|\phi_i\rangle$  the Hamiltonian therefore reads

$$H_0 = - \sum_{i,j} t_{i,j} \sum_{\sigma} c_{i,\sigma}^\dagger c_{j,\sigma} = \sum_{\mathbf{k}} \sum_{\sigma} \varepsilon_{\mathbf{k}} c_{\mathbf{k},\sigma}^\dagger c_{\mathbf{k},\sigma}.$$

The second expression for  $H_0$  is obtained by Fourier transformation

$$c_{\mathbf{k},\sigma}^\dagger = \frac{1}{\sqrt{N}} \sum_j e^{i\mathbf{k}\cdot\mathbf{R}_j} c_{j,\sigma}^\dagger \Rightarrow \varepsilon_{\mathbf{k}} = -\frac{1}{N} \sum_{i,j} t_{i,j} e^{i\mathbf{k}\cdot(\mathbf{R}_i - \mathbf{R}_j)} = - \sum_{\mathbf{R}} t_{\mathbf{R}} e^{i\mathbf{k}\cdot\mathbf{R}}. \quad (1)$$

Here  $\mathbf{k} = (2n\pi/L, 2m\pi/L)$  with integer  $m$  and  $n$  such that  $-L/2 < m, n \leq L/2$  is a wave vector in the first Brillouin zone. Unless otherwise stated we will from now on assume that  $t_{i,j}$  is different from zero only for nearest neighbors  $i$  and  $j$  and denote its value by  $t$ , whence  $\varepsilon_{\mathbf{k}} = -2t(\cos(k_x) + \cos(k_y))$ . The number of wave vectors  $\mathbf{k}$  equals  $N$  and the ground state for  $N$  electrons is obtained by ‘filling the band from below’, that means occupying those  $N/2$  wave vectors  $\mathbf{k}$  which minimize the sum  $\sum_{\mathbf{k}} \varepsilon_{\mathbf{k}}$  with two electrons of opposite spin. The band therefore is half-filled, the Fermi surface covers precisely half of the Brillouin zone and we have a metal.

In the discussion so far we have ignored the Coulomb interaction between the electrons. Recalling that the atomic orbital  $\langle\mathbf{r}|\phi_i\rangle \propto e^{-|\mathbf{r} - \mathbf{R}_i|/\zeta}$ , we expect that if the orbital is occupied by two electrons of opposite spin, the electrostatic energy is  $U \propto e^2/\zeta$ , whereas it is  $V \propto e^2/a$  if the

electrons are in orbitals on different sites. If we take the limit of a ‘small atomic orbital’,  $\zeta \rightarrow 0$ , we find  $U/t \rightarrow \infty$  and  $V/U \rightarrow 0$  whence we neglect the Coulomb repulsion between electrons in different orbitals. Taking the extreme limit  $U \rightarrow \infty$  while  $t$  being fixed, and returning to the problem of finding the ground state with  $N$  electrons we find that there is precisely one electron in each of the  $N$  orbitals (putting two electrons into the same orbital increases the energy by the large amount  $U$ ). The electrons thus are ‘frozen in’ and cannot react to an applied electric field, so that the system is an insulator. This is the prototype of a *Mott insulator*: a system which would be a metal in the band picture, but is an insulator due to the strong Coulomb repulsion between electrons in ‘small’ atomic orbitals. It should be noted that for noninteracting electrons ( $U = 0$ ) and  $t = 0$  the electrons would be unable to move as well and the system would be an insulator. However, any arbitrarily small value of  $t$  would immediately lead to the formation of a band and a Fermi surface, whereas in the presence of a large  $U$  switching on  $t \ll U$  still would not change the insulating nature of the ground state. Let us now try to put these qualitative considerations into a more quantitative form – the famous Hubbard-I approximation.

## 2 The basic concept: Hubbard-I approximation

This is the ‘defining approximation’ of the Mott-insulator by which Hubbard for the first time introduced central concepts of strongly correlated electron systems such as the two Hubbard bands [2]. In the following we give a somewhat sloppy re-derivation of Hubbard’s theory which is meant to clarify its the physical content.

We consider the of infinite  $U$  and  $N_\uparrow = N_\downarrow = N/2$  so that  $N_e = N$ . The ground state has one electron per lattice site and the energy is  $E = 0$ . The way in which the spins are distributed over the sites is not determined, however, rather the number of ways to distribute the  $\uparrow$ -spins (which automatically fixes the  $\downarrow$ -spins) is

$$n_d = \binom{N}{N_\uparrow} \approx \sqrt{\frac{2}{\pi N}} 2^N, \quad (2)$$

where the Stirling formula has been used. This shows the enormous degree of degeneracy. We ignore this degeneracy, however, and assume that there is a unique state  $|\Psi_0\rangle$  which may be thought of as a suitable superposition of all these  $n_d$  degenerate states and which we assume to be ‘disordered’ — it will become clear in a moment what this means.

Next we assume that  $U$  is gradually reduced from infinity. Then, a term in the kinetic energy such as  $t_{i,j} c_{i,\sigma}^\dagger c_{j,\sigma}$  can transfer an electron of spin  $\sigma$  from site  $j$  to another site  $i$  resulting in an empty site at  $j$  and a double occupancy at site  $i$ , whereby the double occupancy increases the energy by  $U$ . The hopping process is possible only if the electron which was originally at the site  $i$  has the spin  $-\sigma$  and since our initial state  $|\Psi_0\rangle$  is ‘disordered’ the probability for this to be the case is  $1/2$  — which is our definition of ‘disordered’. We now interpret the original state  $|\Psi_0\rangle$  as the vacuum state  $|0\rangle$  of our theory and the state created by the hopping process as containing a fermionic hole-like particle at  $j$  and a fermionic double-occupancy-like particle at site  $i$ :  $d_{i,\sigma}^\dagger h_{j,-\sigma}^\dagger |0\rangle$ . The order of the fermionic operators in this state is due to the fact that in the

original hopping term the annihilation operator  $c_{j,\sigma}$  which creates the hole stands to the right of the creation operator  $c_{i,\sigma}^\dagger$  which creates the double occupancy. Moreover we assign the negative spin to the operator which creates the hole because replacement of, e.g., an  $\uparrow$ -electron by a hole decreases the  $z$ -spin by  $1/2$ . We arrive at the following effective Hamiltonian to describe the holes and double occupancies

$$H_{eff,1} = \frac{1}{2} \sum_{i,j} \sum_{\sigma} \left( t_{i,j} d_{i,\sigma}^\dagger h_{j,-\sigma}^\dagger + H.c. \right) + U \sum_{i,\sigma} d_{i,\sigma}^\dagger d_{i,\sigma}. \quad (3)$$

Once a hole and a double occupancy have been created, each of these particles may be transported further by the hopping term. If we assume that the surplus or missing electron retains its spin, which means that the double occupancies and holes propagate without ‘leaving a trace’ of inverted spins, for example a surplus  $\uparrow$ -electron can hop from site  $i$  to site  $j$  only if the spin at site  $j$  is  $\downarrow$  — again we assume that the probability for this is  $1/2$ . We therefore can write down the missing terms for the effective Hamiltonian

$$H_{eff,2} = \frac{1}{2} \sum_{i,j} \sum_{\sigma} t_{i,j} \left( d_{i,\sigma}^\dagger d_{j,\sigma} - h_{i,-\sigma}^\dagger h_{j,-\sigma} \right). \quad (4)$$

The negative sign of the hopping term for holes is due to the fact that the original hopping term has to be rewritten as  $-t_{i,j} c_{j,\sigma} c_{i,\sigma}^\dagger$  to describe the propagation of a hole. Addition of (3) and (4) and Fourier transformation gives

$$H_{eff} = \sum_{\mathbf{k},\sigma} \left( \left( \frac{\varepsilon_{\mathbf{k}}}{2} + U \right) d_{\mathbf{k},\sigma}^\dagger d_{\mathbf{k},\sigma} - \frac{\varepsilon_{\mathbf{k}}}{2} h_{\mathbf{k},\sigma}^\dagger h_{\mathbf{k},\sigma} \right) + \sum_{\mathbf{k},\sigma} \frac{\varepsilon_{\mathbf{k}}}{2} \left( d_{\mathbf{k},\sigma}^\dagger h_{-\mathbf{k},-\sigma}^\dagger + H.c. \right), \quad (5)$$

with  $\varepsilon_{\mathbf{k}}$  given in Eq. (1). Note that this now is a quadratic form where the Coulomb interaction is described by the extra energy of  $U$  for the double-occupancy-like fermion. We make the *ansatz*

$$\begin{aligned} \gamma_{\mathbf{k},+,\sigma}^\dagger &= u_{\mathbf{k}} d_{\mathbf{k},\sigma}^\dagger + v_{\mathbf{k}} h_{-\mathbf{k},-\sigma}, \\ \gamma_{\mathbf{k},-,\sigma}^\dagger &= -v_{\mathbf{k}} d_{\mathbf{k},\sigma}^\dagger + u_{\mathbf{k}} h_{-\mathbf{k},-\sigma}, \end{aligned} \quad (6)$$

and demand that the Hamiltonian takes the form

$$H_{eff} = \sum_{\mathbf{k},\sigma} \left( E_{\mathbf{k},+} \gamma_{\mathbf{k},+,\sigma}^\dagger \gamma_{\mathbf{k},+,\sigma} + E_{\mathbf{k},-} \gamma_{\mathbf{k},-,\sigma}^\dagger \gamma_{\mathbf{k},-,\sigma} \right). \quad (7)$$

We find (with  $W_{\mathbf{k}} = \sqrt{\varepsilon_{\mathbf{k}}^2 + U^2}$ )

$$E_{\mathbf{k},\pm} = \frac{1}{2} (\varepsilon_{\mathbf{k}} + U \pm W_{\mathbf{k}}), \quad u_{\mathbf{k}} = \sqrt{\frac{W_{\mathbf{k}} + U}{2W_{\mathbf{k}}}}, \quad v_{\mathbf{k}} = \frac{\varepsilon_{\mathbf{k}}}{\sqrt{2W_{\mathbf{k}}(W_{\mathbf{k}} + U)}}. \quad (8)$$

In the limit  $U/t \gg 1$  this simplifies to  $E_{\mathbf{k},-} = \varepsilon_{\mathbf{k}}/2$ ,  $E_{\mathbf{k},+} = \varepsilon_{\mathbf{k}}/2 + U$  so that the original band with dispersion  $\varepsilon_{\mathbf{k}}$  is split into two bands, separated by a gap of  $U$  and each having half of the original width. To find out the occupation of the bands, and hence the nature of the Fermi

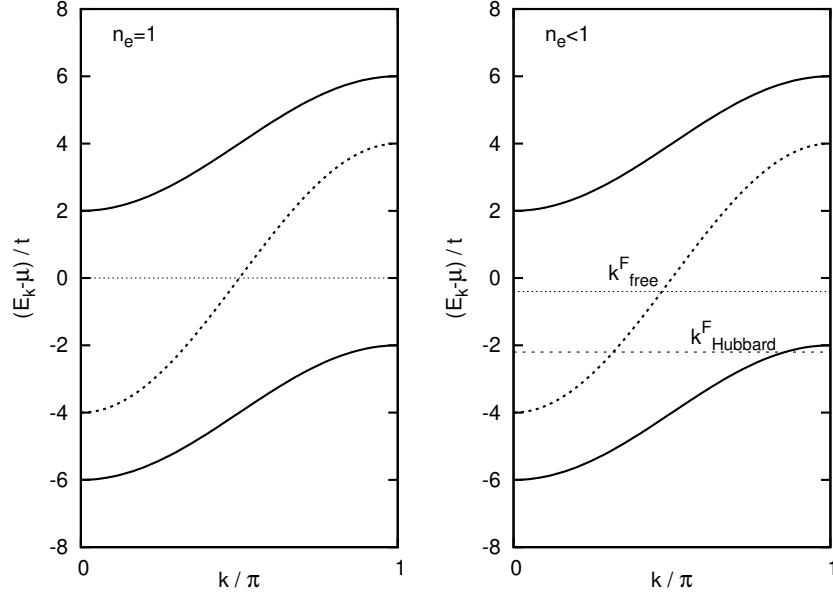


**Fig. 1:** Band structures  $E_{\mathbf{k}}$  for the noninteracting system (dashed line) and from the Hubbard-I approximation ( $U/t = 8$ ). The energies are plotted for  $\mathbf{k} = (k, k)$ , i.e., along the  $(1, 1)$ -direction. For  $n_e = 1$  the half-filled noninteracting band is replaced by the two Hubbard bands, the chemical potential  $\mu$  is in the center of the gap between the two Hubbard bands so that the lower one is completely filled, the upper empty.

For  $n_e < 1$  the noninteracting band becomes less than half-filled, the chemical potential cuts into the top of the lower Hubbard band, forming a hole pocket around  $(\pi, \pi)$ . Note the strong discrepancy of the Fermi wave vectors  $\mathbf{k}^F$ .

surface, we need to count electrons. The vacuum state  $|\Psi_0\rangle$  has one electron per site, i.e., a total of  $N$  electrons. Each double occupancy increases the electron number by one, each hole decreases it by one so that the operator of electron number becomes

$$N_e = N + \sum_{i,\sigma} \left( d_{i,\sigma}^\dagger d_{i,\sigma} - h_{i,\sigma}^\dagger h_{i,\sigma} \right) = \sum_{\mathbf{k},\sigma} \left( d_{\mathbf{k},\sigma}^\dagger d_{\mathbf{k},\sigma} + h_{-\mathbf{k},-\sigma}^\dagger h_{-\mathbf{k},-\sigma} \right) - N.$$

On going over to the expression on the extreme right we have switched to Fourier transforms and assumed fermion anticommutation relations to hold for the  $h_{\mathbf{k},\sigma}^\dagger$ . We note that in the basis  $(d_{\mathbf{k},\sigma}^\dagger, h_{-\mathbf{k},-\sigma})$  the operator matrix for the expression in brackets is the unit matrix which is invariant under unitary transformations whence  $N_e$  also can be written as

$$N_e = \sum_{\mathbf{k},\sigma} \left( \gamma_{\mathbf{k},-\sigma}^\dagger \gamma_{\mathbf{k},-\sigma} + \gamma_{\mathbf{k},+\sigma}^\dagger \gamma_{\mathbf{k},+\sigma} \right) - N. \quad (9)$$

Demanding  $\langle N_e \rangle = N$  the lower band  $E_{\mathbf{k},-}$  must be completely filled whereas the upper band  $E_{\mathbf{k},+}$  must be completely empty, i.e., the chemical potential must be in the center of the gap between lower and upper band see Figure 1. Namely in this case the expectation value of the term in brackets is  $2N$ . Rather than being a metal, as expected for the situation of a half-filled band, the presence of the Coulomb interaction turns the system into an insulator – and this is precisely the definition of the Mott-insulator.

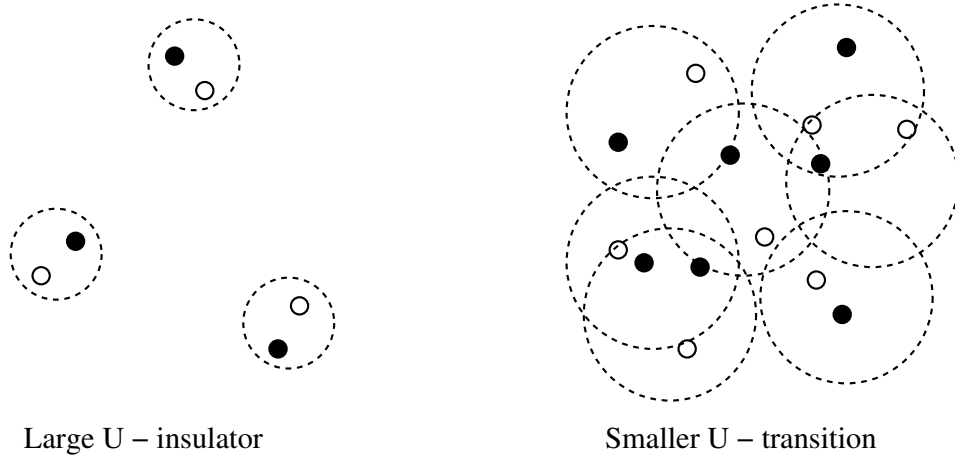


**Fig. 2:** As the ratio  $U/t$  decreases more and more hole-double occupancy pairs are generated and the extent of the pairs increases. At a certain ratio of  $U/t$  the pairs overlap significantly and the phase transition to the metal occurs.

It follows that the ground state wave function  $|\Phi_0\rangle$  must obey  $\gamma_{\mathbf{k},-\sigma}^\dagger|\Phi_0\rangle = \gamma_{\mathbf{k},+\sigma}|\Phi_0\rangle = 0$ . This can be achieved by choosing

$$|\Phi_0\rangle = \prod_{\mathbf{k},\sigma} \left( u_{\mathbf{k}} + v_{\mathbf{k}} h_{-\mathbf{k},-\sigma}^\dagger d_{\mathbf{k},\sigma}^\dagger \right) |\Psi_0\rangle \propto e^{\sum_{\mathbf{k},\sigma} \frac{v_{\mathbf{k}}}{u_{\mathbf{k}}} h_{-\mathbf{k},-\sigma}^\dagger d_{\mathbf{k},\sigma}^\dagger} |\Psi_0\rangle.$$

The similarity with the BCS wave function shows that  $|\Phi_0\rangle$  may be viewed as the original background  $|\Psi_0\rangle$ , which has one electron per site and is spin-disordered, populated by electron-hole pairs. The expression in the exponent is

$$\sum_{\mathbf{k},\sigma} \frac{v_{\mathbf{k}}}{u_{\mathbf{k}}} h_{-\mathbf{k},-\sigma}^\dagger d_{\mathbf{k},\sigma}^\dagger = \sum_{i,\mathbf{R}} f(\mathbf{R}) h_{\mathbf{R}_i,-\sigma}^\dagger d_{\mathbf{R}_i+\mathbf{R},\sigma}^\dagger \quad \text{with} \quad f(\mathbf{R}) = \frac{1}{N} \sum_{\mathbf{k}} \frac{v_{\mathbf{k}}}{u_{\mathbf{k}}} e^{i\mathbf{k}\mathbf{R}} \xrightarrow{U \rightarrow \infty} \frac{t}{U} \delta_{|\mathbf{R}|,1}.$$

This shows that for large  $U$  the density of pairs is  $\propto (t/U)^2$  and the double-occupancy and the hole are almost exclusively on nearest neighbors.

If in a *gedankenexperiment* one would reduce the value of  $U$  starting from  $U = \infty$ , one would expect that, as  $U$  decreases, both the density of such pairs would increase and the diameter of a pair would increase, see Figure 2. If  $U$  becomes sufficiently low the pairs start to overlap and at that point the entire picture is likely to break down so we have the insulator-to-metal transition. Viewed that way one might conjecture that the order parameter for the insulator-to-metal transition is the double occupancy-hole pairing amplitude  $\langle d_{\mathbf{k},\sigma}^\dagger h_{-\mathbf{k},-\sigma}^\dagger \rangle$ . Does the Hubbard-I approximation describe such a transition to the metallic state? The simplest way to answer this question is to consider the gap between the upper and lower Hubbard band in the limit  $U/t \rightarrow 0$ . One finds

$$\Delta = E_{\mathbf{k}=(0,0),+} - E_{\mathbf{k}=(\pi,\pi),-} \propto \frac{U^2}{4t},$$

where the extreme right-hand-side holds for  $U \rightarrow 0$ . This shows that there is a gap even for arbitrarily small  $U$ , i.e., there is no insulator-to-metal transition with decreasing  $U$  in the Hubbard-I approximation.

Next, what would happen if we reduce the electron number  $N_e$  from  $N \rightarrow (1-\delta)N$ , i.e., we ‘dope the Mott insulator’? First, one would assume that all the factors of  $1/2$  in the above derivation should be replaced by  $(1-\delta)/2$  because this is now the probability that on any given site there is an electron with a given spin  $\sigma$ . This will lead to only a slight modification of the quasiparticle dispersion. More importantly, however, the occupation of the lower Hubbard band will be reduced. Inspection of (9) shows that now

$$\left\langle \sum_{\mathbf{k},\sigma} \left( \gamma_{\mathbf{k},-,\sigma}^\dagger \gamma_{\mathbf{k},-,\sigma} + \gamma_{\mathbf{k},+,\sigma}^\dagger \gamma_{\mathbf{k},+,\sigma} \right) \right\rangle = (2-\delta)N,$$

so that the occupied part of the lower Hubbard band must now contain  $N_{Hubbard} = (1-\delta/2)N$  momenta  $\mathbf{k}$ . This means that  $N\delta/2$   $\mathbf{k}$ -points must be unoccupied so that the Fermi surface is a small hole-pocket around the top of the lower Hubbard band at  $\mathbf{k} = (\pi, \pi)$ , see Figure 1. Compare this to the noninteracting case,  $U = 0$  where the occupied part of the band contains  $N_{free} = ((1-\delta)/2)N$  momenta, whence the difference  $N_{Hubbard} - N_{free} = N/2$ . If we assume that the Hubbard-I approximation is at least qualitatively correct for the lightly doped Mott-insulator, i.e., small  $\delta$ , this immediately leads to an interesting question: namely for low electron density  $n_e \ll 1$  one recovers the noninteracting Fermi surface even for arbitrarily large  $U$  [3]. The reason is that for low electron density the probability for collisions between electrons is small and the interaction becomes largely irrelevant. Accordingly, if one gradually reduces the electron number starting from  $n_e = 1$  one would expect that one first has the Fermi surface with a volume  $\propto \delta/2$  as predicted by the Hubbard-I approximation but at a certain critical  $n_e$  the Fermi surface volume must change to the free-electron value of  $(1-\delta)/2$ , i.e., a phase transition between two phases with different Fermi surface volume with increasing doping. An obvious candidate for this phase transition would be the enigmatic quantum critical point in cuprate superconductors which gives rise to the superconducting dome in these compounds.

Finally let us address a subtle problem which actually is related to a very fundamental problem in strongly correlated electrons. In the above discussion we have assigned a spin to the holes and double occupancies:  $d_{i,\sigma}^\dagger$  and  $h_{j,\sigma}^\dagger$ . However, both an empty site and a doubly occupied site are spinless objects! On the other hand, if the vacuum state  $|\Psi_0\rangle$  has a definite  $z$ -spin  $S_z$ , the states  $c_{i,\uparrow}|\Psi_0\rangle$  and  $c_{i,\downarrow}|\Psi_0\rangle$  are orthogonal to each other because they have  $S_z \mp 1/2$ . This is despite the fact that the empty site at  $i$  is a spinless object. The information whether an  $\uparrow$ -electron or a  $\downarrow$ -electron has been removed from site  $i$  therefore must be ‘stored’ somewhere else in the resulting state. If one now were to remove an electron at site  $i$  and subsequently let the resulting state evolve under the action of the Hamiltonian one can take two different points of view: when the empty site propagates, the information about the spin of the removed electron may ‘stay in the neighborhood’ of the spinless vacancy, so that effectively there is a spin- $1/2$  particle propagating. Obviously, in the Hubbard-I approximation one is implicitly assuming just this. Alternatively one might assume that the spinless vacancy and the ‘spin information’ acquire an independent existence and separate from each other, a scenario often referred to as spin-charge separation.

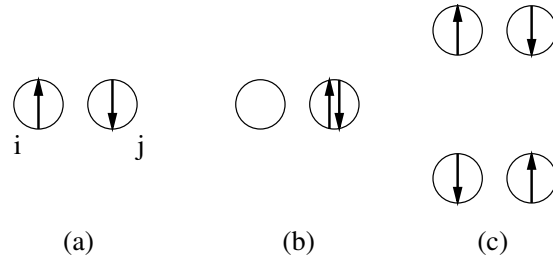


**Fig. 3:** An exchange process in a Mott insulator.

### 3 Antiferromagnets

#### 3.1 Spin exchange

In the introduction we have already mentioned one of the reasons why the problem of the Mott-insulator is so difficult. Whereas the ground state for  $N_e = N$  and  $U = 0$  is unique and easy to write down – the half-filled Fermi sea – a well-defined ground state for  $U/t = \infty$  does not even exist. Rather, the ground state is highly degenerate, see equation (2) above. In the Hubbard-I approximation we have bypassed this problem by assuming that there is a unique ‘disordered’ ground state of  $N$  electrons on  $N$  sites, and that the only active degrees of freedom are the double-occupancies and holes. This, however, ignores the possibility of *spin exchange*. If we reduce  $U/t$  from infinity to a large but finite value, the spins on the individual sites start to ‘communicate’ with each other via the process shown in Figure 3. An electron from site  $i$  may hop to a neighbor  $j$  and form an intermediate state with an empty orbital at  $i$  and a doubly occupied orbital at  $j$ , see Figure 3(b). Since the energy of this intermediate state is  $U$ , it will be short lived and one of the two electrons in  $j$  will hop to the empty site  $i$ , resulting in one of the two states in Figure 3(c). The upper state is identical to the initial state, Figure 3(a), but there is a gain in kinetic energy of order  $t^2/U$  due to the back-and-forth hopping of the electron. Since this back-and-forth hopping is possible only if the spins at  $i$  and  $j$  are antiparallel to each other, it is energetically favorable if spins on nearest neighbors are antiparallel. In the lower of the two states in Figure 3(c) both spins have flipped their direction as compared to Figure 3(a), so that the spins in the Mott insulator are not static, but have a dynamics of their own. A more quantitative treatment shows [4] that the ‘virtual’ hopping processes in Figure 3 can be described by the *Heisenberg antiferromagnet*

$$H_{HAF} = J \sum_{\langle i,j \rangle} \mathbf{S}_i \cdot \mathbf{S}_j = J \sum_{\langle i,j \rangle} \left( S_i^z S_j^z + \frac{1}{2} (S_i^+ S_j^- + S_i^- S_j^+) \right). \quad (10)$$

Here  $J = 4t^2/U$  while  $\sum_{\langle i,j \rangle}$  denotes a sum over all  $2N$  nearest neighbor pairs, and  $\mathbf{S}_i$  is the operator of electron spin at site  $i$  and the spin raising and lowering operators  $S^\pm = S_x \pm iS_y$  have been introduced to rewrite the term  $S_{i,x}S_{j,x} + S_{i,y}S_{j,y}$ . We see that although the electrons in a Mott insulator are localized, their spins acquire a ‘life of their own’, resulting in a magnetic ground state and a spectrum of *spin-excitations*.

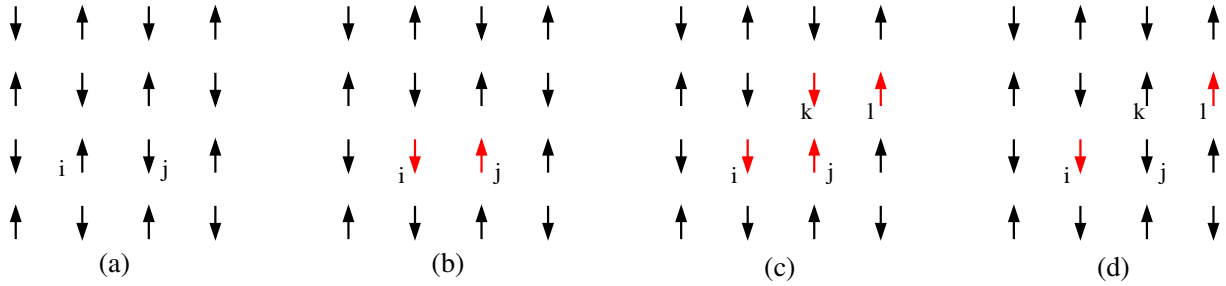


**Fig. 4:** The Néel state (a) is not the ground state of the Heisenberg antiferromagnet. By acting, e.g., with the term  $\frac{J}{2} S_i^- S_j^+$  in (10) the state (b) is generated, which is orthogonal to the Néel state. Acting further with  $\frac{J}{2} S_k^- S_l^+$  produces (c) and then acting with  $\frac{J}{2} S_j^- S_k^+$  gives (d).

### 3.2 Magnons in an antiferromagnet

We consider the undoped Mott insulator,  $N_e = N$ , and assume that the spins degrees of freedom of the electrons are described by the Heisenberg antiferromagnet, Eq. (10). If only the terms  $\propto S_i^z S_j^z$  were present, the ground state of (10) would be the Néel state, shown in Figure 4(a). In this state, the square lattice is divided into two *sublattices* whereby all sites of the *A*-sublattice are occupied by an  $\uparrow$ -electron, those of the *B*-sublattice by a  $\downarrow$ -electron (we assume that the *A*-sublattice is the one containing the site  $(0, 0)$ ). The energy of this state is  $2N \cdot (-J/4) = -NJ/2$ . The Néel state, however, is not an eigenstate of the full Hamiltonian (10): acting, e.g., with one of the products  $\frac{J}{2} S_i^- S_j^+$  contained in the second term in (10), the spins at the sites  $i$  and  $j$  are inverted, resulting in the state shown in Figure 4(b) which is orthogonal to the Néel state. Interestingly, the inverted spins have very much the character of particles in that they can propagate: first, the term  $\frac{J}{2} S_k^- S_l^+$  appends two additional inverted spins, see Figure 4(c), and then the term  $\frac{J}{2} S_j^- S_k^+$  removes two inverted spins, to produce the state in Figure 4(d). The net result of this two-step process is that one of the inverted spins seems to have moved from site  $j$  to site  $l$ . The particle-like nature of the inverted spins has led to the name *magnons* for them. One can then envisage how this will go on: magnons are created in pairs at various places in the system, then separate and propagate independently by the append-and-remove process, but when two magnons meet they can also ‘pair-annihilate’ each other by the inverse process Figure 4(b)  $\rightarrow$  (a). There are then two possible outcomes of this scenario: the density of magnons may reach an equilibrium value, where pair-creation and pair annihilations balance each other, so that the underlying antiferromagnetic order persists and we have a Néel state hosting a ‘gas of magnons’, or the process may go on until the ordered state is wiped out and we get an entirely new state without order. It turns out that in dimensions  $D \geq 2$  the first scenario is realized, and the resulting gas of magnons in antiferromagnetic Mott insulators can be described very well by *linear spin wave theory*. This is frequently derived by means of the Holstein-Primakoff transformation [5] but for the extreme quantum limit of spin  $1/2$ , which we are considering here, a simpler and more transparent derivation is possible.

We interpret the Néel state in Figure 4(a) as the vacuum state  $|0\rangle$  for magnons and model an inverted spin at the site  $i$  of the *A* sublattice by the presence of a boson, created by  $a_i^\dagger$ . Similarly, an inverted spin on the site  $j$  of the *B* sublattice is modeled by the presence of a boson created

by  $b_j^\dagger$ . The state in Figure 4(b) thus would be represented as  $a_i^\dagger b_j^\dagger |0\rangle$ . We use bosons to represent the magnons because spin-flip operators such as  $S_i^+$  and  $S_j^-$  commute for different sites  $i$  and  $j$  and these are the operators which create or annihilate the magnons. Since any given spin can be inverted only once, a state like  $(a_i^\dagger)^2 |0\rangle$  is meaningless. Accordingly, we have to impose the constraint that at most one boson can occupy a given site. This is equivalent to an infinitely strong on-site repulsion between the magnons and we call this the *hard-core constraint*. An inverted spin on either sublattice is parallel to its  $z = 4$  nearest neighbors and the energy changes from  $-J/4$  to  $+J/4$  for each of these  $z$  bonds. Accordingly, we ascribe an energy of formation of  $zJ/2$  to each boson. The spin-flip part creates or annihilates pairs of magnons on nearest neighbors, with the matrix element being  $J/2$ , so that the Hamiltonian for the magnons becomes

$$H_{SW} = \frac{zJ}{2} \left( \sum_{i \in A} a_i^\dagger a_i + \sum_{i \in B} b_i^\dagger b_i \right) + \frac{J}{2} \sum_{i \in A} \sum_{\mathbf{n}} \left( a_i^\dagger b_{i+\mathbf{n}}^\dagger + b_{i+\mathbf{n}} a_i \right). \quad (11)$$

Here  $\mathbf{n}$  are the  $z$  vectors which connect a given site with its  $z$  nearest neighbors. Note that when two inverted spins reside on nearest neighbors, the number of frustrated bonds is  $2(z-1)$  rather than  $2z$ . This could be incorporated into  $H_{SW}$  as an attractive interaction between magnons on nearest neighbors, but here we ignore this.

The Hamiltonian (11) is a quadratic form but we recall that the bosons are not free particles, but have to obey the hard-core constraint. However, for the moment we ignore this and treat the bosons as if they were noninteracting – we will return to this issue later on. Fourier transformation of (11) gives

$$\begin{aligned} H_{SW} &= \frac{zJ}{2} \sum_{\mathbf{k}} \left( a_{\mathbf{k}}^\dagger a_{\mathbf{k}} + b_{\mathbf{k}}^\dagger b_{\mathbf{k}} + \gamma_{\mathbf{k}} (a_{\mathbf{k}}^\dagger b_{-\mathbf{k}}^\dagger + b_{-\mathbf{k}} a_{\mathbf{k}}) \right), \\ a_{\mathbf{k}}^\dagger &= \sqrt{\frac{2}{N}} \sum_{j \in A} e^{i\mathbf{k} \cdot \mathbf{R}_j} a_j^\dagger, \\ \gamma_{\mathbf{k}} &= \frac{1}{z} \sum_{\mathbf{n}} e^{i\mathbf{k} \cdot \mathbf{n}} = \frac{1}{4} (2 \cos(k_x) + 2 \cos(k_y)), \end{aligned} \quad (12)$$

where  $\mathbf{k}$  is a wave vector in the antiferromagnetic Brillouin zone (AFBZ), see Figure 5. We can diagonalize (12) by a *bosonic Bogoliubov transformation*, i.e., we make the ansatz

$$\begin{aligned} \alpha_{\mathbf{k}}^\dagger &= u_{\mathbf{k}} a_{\mathbf{k}}^\dagger + v_{\mathbf{k}} b_{-\mathbf{k}}, & \Rightarrow & & \alpha_{\mathbf{k}}^\dagger &= u_{\mathbf{k}} \alpha_{\mathbf{k}}^\dagger - v_{\mathbf{k}} \beta_{-\mathbf{k}}, \\ \beta_{-\mathbf{k}}^\dagger &= u_{\mathbf{k}} b_{-\mathbf{k}}^\dagger + v_{\mathbf{k}} a_{\mathbf{k}}, & & & b_{-\mathbf{k}} &= -v_{\mathbf{k}} \alpha_{\mathbf{k}}^\dagger + u_{\mathbf{k}} \beta_{-\mathbf{k}}. \end{aligned} \quad (13)$$

Demanding that  $[\alpha_{\mathbf{k}}, \alpha_{\mathbf{k}}^\dagger] = [\beta_{\mathbf{k}}, \beta_{\mathbf{k}}^\dagger] = 1$  gives the condition  $u_{\mathbf{k}}^2 - v_{\mathbf{k}}^2 = 1$ , which actually has been used to revert the equations on the left hand side of (13) to obtain the right hand side. Next, we demand that when expressed in terms of the  $\alpha_{\mathbf{k}}^\dagger$  and  $\beta_{\mathbf{k}}^\dagger$  the Hamiltonian takes the form

$$H = \sum_{\mathbf{k}} \omega_{\mathbf{k}} (\alpha_{\mathbf{k}}^\dagger \alpha_{\mathbf{k}} + \beta_{\mathbf{k}}^\dagger \beta_{\mathbf{k}}) + \text{const},$$

which implies that  $[H, \alpha_{\mathbf{k}}^\dagger] = \omega_{\mathbf{k}} \alpha_{\mathbf{k}}^\dagger$ . We now insert the *ansatz* (13) into this equation, use the bosonic commutation relations for  $a^\dagger$  and  $b^\dagger$ , and equate the coefficients of  $\alpha_{\mathbf{k}}^\dagger$  and  $b_{-\mathbf{k}}$  on both

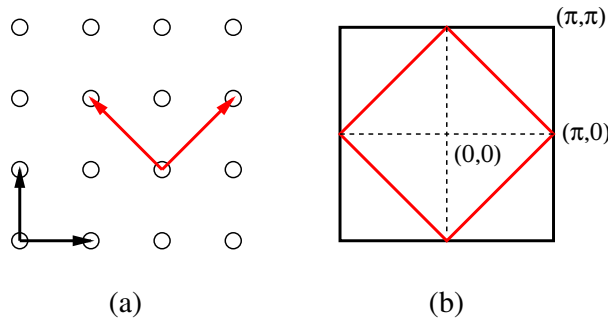


**Fig. 5:** (a) The ordered moments in the Néel state make the two sublattices inequivalent, so that the new lattice vectors connect only the sites of one sublattice. The new unit cell is rotated by  $45^\circ$  and has twice the size of the original one. (b) Accordingly, the new Brillouin zone is rotated by  $45^\circ$  as well and has half the size of the original one.

sides of the resulting equation. This leads to the following non-Hermitian eigenvalue problem:

$$\begin{pmatrix} zJ/2 & -\gamma_{\mathbf{k}} \\ \gamma_{\mathbf{k}}^* & -zJ/2 \end{pmatrix} \begin{pmatrix} u_{\mathbf{k}} \\ v_{\mathbf{k}} \end{pmatrix} = \omega_{\mathbf{k}} \begin{pmatrix} u_{\mathbf{k}} \\ v_{\mathbf{k}} \end{pmatrix}. \quad (14)$$

The eigenvalues and eigenvectors of (14) are easily calculated and one finds

$$\omega_{\mathbf{k}} = \frac{zJ}{2} \sqrt{1-\gamma_{\mathbf{k}}^2}, \quad u_{\mathbf{k}} = \sqrt{\frac{1+\nu_{\mathbf{k}}}{2\nu_{\mathbf{k}}}}, \quad \text{and} \quad v_{\mathbf{k}} = \sqrt{\frac{1-\nu_{\mathbf{k}}}{2\nu_{\mathbf{k}}}}, \quad (15)$$

where  $\nu_{\mathbf{k}} = \sqrt{1-\gamma_{\mathbf{k}}^2}$ . In particular, for  $\mathbf{k} \rightarrow 0$  we find  $\gamma_{\mathbf{k}} \rightarrow 1 - (k_x^2 + k_y^2)/4 = 1 - \mathbf{k}^2/4$  so that  $\nu_{\mathbf{k}} \rightarrow |\mathbf{k}|/\sqrt{2}$  and  $\omega_{\mathbf{k}} \rightarrow J\sqrt{2}|\mathbf{k}|$ . This shows that the spin waves reach zero frequency at  $\mathbf{k} = (0, 0)$  and have a cone-shaped dispersion in the neighborhood.

Linear spin wave theory is extremely successful in describing many properties of antiferromagnetic Mott-insulators. An example for the experimental observation of magnons by inelastic neutron scattering and the excellent agreement of the experimental results with linear spin wave theory can be found in Ref. [6].

To conclude this section, we return to the issue of the hard-core constraint which the  $a^\dagger$  and  $b^\dagger$  bosons had to obey and which we had simply ignored. To address this question, we calculate the density of these bosons, i.e.

$$n_a = \frac{2}{N} \sum_{\mathbf{k}} \langle a_{\mathbf{k}}^\dagger a_{\mathbf{k}} \rangle = \frac{2}{N} \sum_{\mathbf{k}} v_{\mathbf{k}}^2 = \frac{2}{N} \sum_{\mathbf{k}} \frac{1-\nu_{\mathbf{k}}}{2\nu_{\mathbf{k}}}.$$

Numerical evaluation for a 2D square lattice gives  $n_a = 0.19$ . The probability that two of the bosons occupy the same site and violate the constraint therefore is  $\approx n_a^2 = 0.04 \ll 1$  and our assumption of relaxing the constraint is justified a posteriori.

Summarizing the discussion so far we have seen that in a Mott-insulator the sites carry a spin of  $\pm 1/2$ . These spins can communicate with each other by means of virtual charge fluctuations and this is described by the Heisenberg antiferromagnet. In dimensions  $D \geq 2$  this leads to antiferromagnetic order in the ground state and a new type of excitations, magnons or spin waves, which correspond to spins standing opposite to the antiferromagnetic order and these inverted spins propagate through the lattice. In the next section we investigate how the doped holes interact with these spin excitations.

### 3.3 One hole in an antiferromagnet

We have seen that in a Mott insulator ‘virtual’ hopping processes lead to a coupling of spins which results in antiferromagnetic order and spin excitations. In this section we study the first step towards the ‘doped’ the Mott insulator and consider a single hole in an antiferromagnet. A single hole will not destroy the magnetic order due to the Heisenberg exchange between the remaining  $N-1$  spins so we continue to assume antiferromagnetic order. The appropriate model to describe such a system is the famous  $t$ - $J$  model

$$H_{t,J} = -t \sum_{\langle i,j \rangle} \sum_{\sigma} (\hat{c}_{i,\sigma}^{\dagger} \hat{c}_{j,\sigma} + H.c.) + J \sum_{\langle i,j \rangle} \mathbf{S}_i \cdot \mathbf{S}_j, \quad (16)$$

where the *Hubbard operator*  $\hat{c}_{i,\sigma}^{\dagger} = c_{i,\sigma}^{\dagger}(1-n_{i,\bar{\sigma}})$  creates an electron only on an empty site. The  $t$ - $J$  model was originally derived rigorously as the strong coupling version of the Hubbard model by Chao, Spałek, and Oleś [4]. The model describes the lower Hubbard band — note that the operator  $\hat{c}_{i,\sigma}$  corresponds precisely to the operator  $h_{i,\bar{\sigma}}^{\dagger}$  we used in the Hubbard-I approximation — but augments this by the effect of the Heisenberg exchange. Later it was shown by Zhang and Rice [7] that the  $t$ - $J$  model is also the proper theoretical description of the  $\text{CuO}_2$  planes in cuprate superconductors. For application to the  $\text{CuO}_2$  planes, the appropriate parameter values are  $t \approx 350$  meV and  $J \approx 140$  meV, so  $J/t = 0.4$ . The Hilbert space of the  $t$ - $J$  model consists of states where each site is occupied either by a vacancy or a spin. The first term  $\propto -t$  exchanges a vacancy and a spin on nearest neighbors, the second term  $\propto J$  is the Heisenberg exchange between spins. In order to study the motion of a single hole in an antiferromagnet we decompose the  $t$ - $J$  Hamiltonian Eq. (16) as  $H = H_t + H_I + H_{\perp}$  whereby

$$H_t = -t \sum_{\langle i,j \rangle} \sum_{\sigma} (\hat{c}_{i,\sigma}^{\dagger} \hat{c}_{j,\sigma} + H.c.), \quad H_I = J \sum_{\langle i,j \rangle} S_i^z S_j^z, \quad H_{\perp} = \frac{J}{2} \sum_{\langle i,j \rangle} (S_i^+ S_j^- + H.c.),$$

and choose  $H_0 = H_t + H_I$  as our unperturbed Hamiltonian. As already stated, in the absence of any hole the ground state of  $H_0$  is the Néel state with energy  $E_N = -NJ/2$ . Next assume that an electron is removed from site  $i$  belonging to the  $\uparrow$ -sublattice, see Figure 6(a). This raises the exchange energy by  $zJ/4$ , because  $z$  bonds change their energy from  $-J/4$  to 0. We choose the exchange energy of the resulting state,  $E_N + zJ/4$ , as the zero of energy. Then, the hopping term in (16) can become active and the spin from a neighboring site  $i_1$  is transferred to  $i$ , resulting in the state in Figure 6(b). Since the shifted spin has ‘switched sublattices’, however, it now is opposite to the antiferromagnetic order. In fact, this inverted spin at site  $i$  is nothing but a magnon as discussed in the preceding section, so that the hopping vacancy ‘radiates off’ magnons [8, 9]. Since the displaced spin at site  $i$  is parallel to  $z-1$  neighbors, the exchange energy increases by  $(z-1)J/2$ . And this continues as the vacancy moves through the Néel state, see Figure 6(c): in each step another spin is shifted to the opposite sublattice, so that the vacancy leaves behind a trace of misaligned spins and the exchange energy increases roughly linearly with the distance travelled by the hole. We call a state which is created by the motion of a vacancy in the Néel state a ‘string state’ and denote it by  $|i_0, i_1, \dots, i_{\nu}\rangle$ . Here  $i_0$  is the site

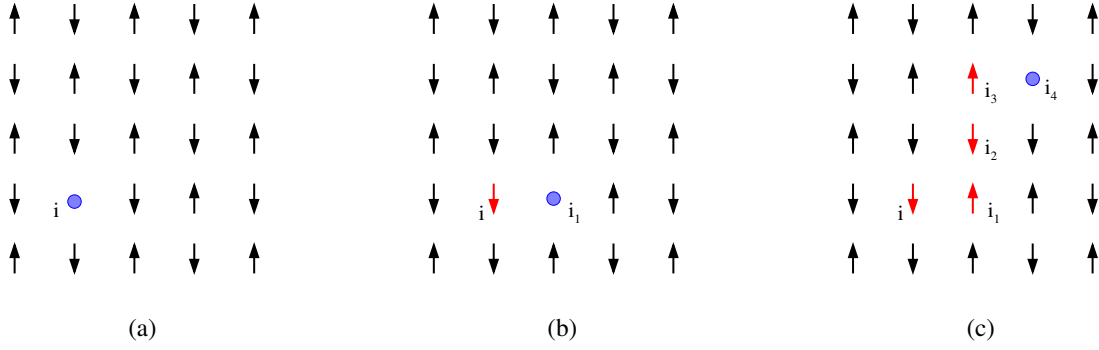


**Fig. 6:** A hole hopping in the Néel state creates a ‘string’ of misaligned spins.

where the hole was created,  $i_1, i_2, i_{\nu-1}$  are the sites visited by the hole, whereas  $i_\nu$  is the site where the vacancy is located. We call  $\nu$  the length of the string, for example Figure 6(c) shows a string of length 4. There are  $z$  different string states with  $\nu = 1$ , whereas in any subsequent hop starting from a string state of length  $\nu$ ,  $z-1$  new string states of length  $\nu+1$  are generated. The number of different strings of length  $\nu$  therefore is  $n_\nu = z(z-1)^{\nu-1}$  for  $\nu \geq 1$  whereas  $n_0 = 1$ . Since each displaced spin is parallel to  $z-2$  neighbors, compare Figure 6, the magnetic energy increases by  $J(z-2)/2$  per displaced spin, except for the first hop away from  $i$  where it increases by  $J(z-1)/2$ . Accordingly, the exchange energy for a string of length  $\nu > 0$  is

$$I_\nu = \frac{(z-1)J}{2} + (\nu-1) \frac{(z-2)J}{2} = \frac{J}{2} ((z-1) + (\nu-1)(z-2)), \quad (17)$$

and  $I_0 = 0$ . It may happen that the path which the hole has taken is folded or self-intersecting in which case (17) clearly is not correct. However it will be correct for ‘most’ possible paths of the hole, in particular it is correct for  $\nu \leq 2$  so that we will use this expression. Neglecting the possibility of self-intersection or folding of the string is an approximation known as *Bethe-lattice*. Since the magnetic energy increases linearly with the number of hops the hole has taken we conclude that under the action of  $H_0$  the hole is self-trapped. To describe the resulting localized state we make the *ansatz*

$$|\Phi_i\rangle = \sum_{\nu=0}^{\infty} \alpha_\nu \sum_{i_1, i_2, \dots, i_\nu} |i, i_1, i_2, \dots, i_\nu\rangle, \quad (18)$$

where it is understood that the second sum runs only over those  $\nu$ -tuples of sites which correspond to a true string starting at  $i$ . Since we assume that the magnetic energy is the same for all strings of length  $\nu$ , the coefficient  $\alpha_\nu$  also depends only on the length of the string. The coefficients  $\alpha_\nu$  in (18) are to be determined by minimizing the expectation value of  $H_0$ . The norm and magnetic energy are

$$\langle \Phi_i | \Phi_i \rangle = \sum_{\nu=0}^{\infty} n_\nu \alpha_\nu^2 = \sum_{\nu=0}^{\infty} \beta_\nu^2, \quad (19)$$

$$\langle \Phi_i | H_I | \Phi_i \rangle = \sum_{\nu=0}^{\infty} n_\nu I_\nu \alpha_\nu^2 = \sum_{\nu=0}^{\infty} I_\nu \beta_\nu^2, \quad (20)$$

where we have introduced  $\beta_\nu = \alpha_\nu / \sqrt{n_\nu}$ .

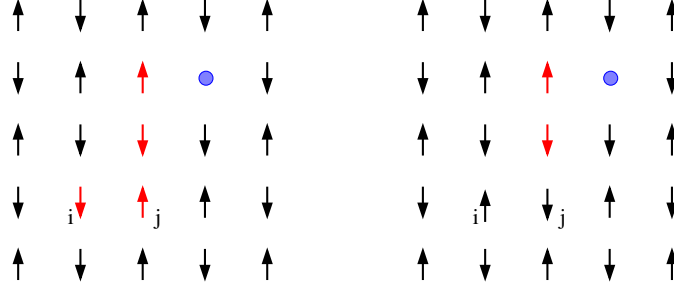


**Fig. 7:** By acting with the term  $\frac{J}{2} S_i^+ S_j^-$  the first two defects created by the hole can be ‘healed’ and the starting point of the string be shifted to a neighbor.

To obtain the expectation value of the kinetic energy we consider a string state of length  $\nu \geq 1$  which has the coefficient  $\alpha_\nu$ . By acting with the hopping term we obtain  $z-1$  strings of length  $\nu+1$ , with coefficient  $\alpha_{\nu+1}$ , and 1 string of length  $\nu-1$ , with coefficient  $\alpha_{\nu-1}$ . For  $\nu = 0$  we obtain  $z$  strings of length 1. In this way we find

$$\langle \Phi_i | H_t | \Phi_i \rangle = t \left( z \alpha_0 \alpha_1 + \sum_{\nu=1}^{\infty} n_\nu \alpha_\nu (\alpha_{\nu-1} + (z-1) \alpha_{\nu+1}) \right) = 2t \sum_{\nu=0}^{\infty} n_{\nu+1} \alpha_\nu \alpha_{\nu+1} = 2 \sum_{\nu=0}^{\infty} \tilde{t}_\nu \beta_\nu \beta_{\nu+1}, \quad (21)$$

where  $\tilde{t}_0 = \sqrt{z} t$  and  $\tilde{t}_\nu = \sqrt{z-1} t$  for  $\nu > 0$ . The prefactor on the right hand side is  $t$  instead of  $-t$  as one might have expected from (16) because the hopping term has to be rearranged as  $-t \hat{c}_{i,\sigma}^\dagger \hat{c}_{j,\sigma} = t \hat{c}_{j,\sigma} \hat{c}_{i,\sigma}^\dagger$  to describe the hopping of a hole. As already stated, the  $\beta_\nu$  now are determined from the requirement that the expectation value  $E_{loc} = \langle \Phi_i | H_0 | \Phi_i \rangle / \langle \Phi_i | \Phi_i \rangle$  be stationary under variation of each  $\beta_\nu$

$$\begin{aligned} \frac{\partial E_{loc}}{\partial \beta_\nu} &= \frac{1}{\langle \Phi_i | \Phi_i \rangle^2} \left[ \frac{\partial \langle \Phi_i | H_0 | \Phi_i \rangle}{\partial \beta_\nu} \langle \Phi_i | \Phi_i \rangle - \langle \Phi_i | H_0 | \Phi_i \rangle \frac{\partial \langle \Phi_i | \Phi_i \rangle}{\partial \beta_\nu} \right] \\ &= \frac{1}{\langle \Phi_i | \Phi_i \rangle} \left[ \frac{\partial \langle \Phi_i | H_0 | \Phi_i \rangle}{\partial \beta_\nu} - E_{loc} \frac{\partial \langle \Phi_i | \Phi_i \rangle}{\partial \beta_\nu} \right] = 0. \end{aligned}$$

Setting the square bracket equal to zero and using Eqs. (19), (20) and (21) we obtain [10]

$$(\tilde{t}_\nu \beta_{\nu+1} + \tilde{t}_{\nu-1} \beta_{\nu-1}) + I_\nu \beta_\nu = E_{loc} \beta_\nu,$$

with the boundary condition  $\beta_{-1} = 0$ . This results in a tridiagonal Hamilton matrix for the  $\beta_\nu$  and after cutting off at a sufficiently large  $\nu$ ,  $E_{loc}$  and the  $\beta_s$  can be obtained by a simple numerical matrix diagonalization.

So far it seems that the hole in the Néel state is localized. It is easy to see, however, that the term  $H_\perp$  which we have neglected so far can assist the trapped hole in escaping from the string potential, see Figure 7. Namely by acting on the first two sites of a string the spins which were inverted by the hole are inverted a second time and thus fit with the Néel order again:  $H_\perp |i, i_1, i_2, i_3, \dots, i_\nu\rangle = J/2 |i_2, i_3, \dots, i_\nu\rangle$ . The initial site of the string thus is shifted to a (2, 0)- or (1, 1)-like neighbor while simultaneously the length  $\nu$  is decreased by two. The term  $H_\perp$  may also append two new defects to a string,  $H_\perp |i_2, i_3, \dots, i_\nu\rangle = J/2 |i, i_1, i_2, i_3, \dots, i_\nu\rangle$

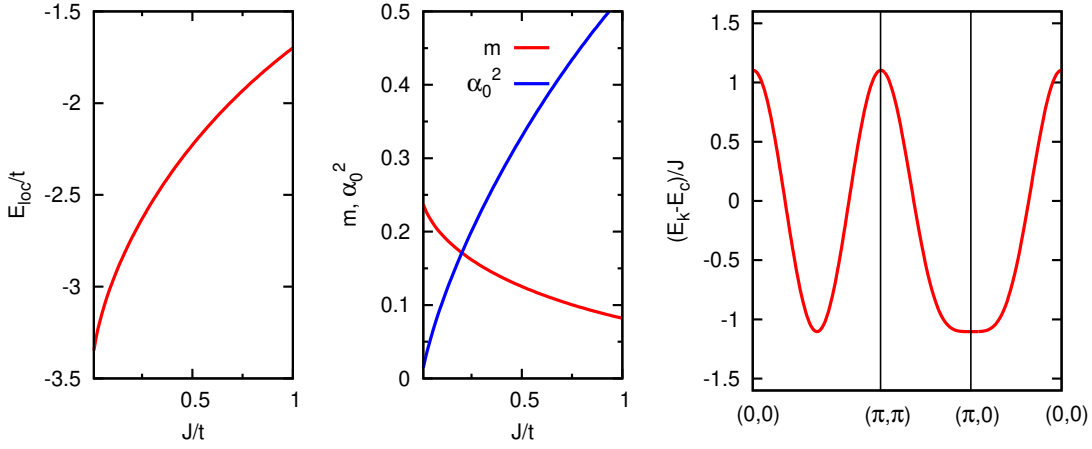


**Fig. 8:** Left: Energy of the self-trapped state  $E_{loc}$  versus  $J/t$ . Center: Matrix element  $m$  due to string truncation and renormalization factor  $\alpha_0^2$  for the  $t'$  and  $t''$  hopping terms versus  $J/t$ . Right: Band structure  $E_k$  for  $J/t = 0.4$ .

thus increasing the length by 2 and again shifting the starting point to a  $(2, 0)$ - or  $(1, 1)$ -like neighbor. Using again the Bethe lattice approximation we find the matrix element

$$\langle \Phi_{i+2\hat{x}} | H_{\perp} | \Phi_i \rangle = J \sum_{\nu=0}^{\infty} (z-1)^{\nu} \alpha_{\nu} \alpha_{\nu+2} = \frac{J}{z} \left( \sqrt{\frac{z}{z-1}} \beta_0 \beta_2 + \sum_{\nu=1}^{\infty} \beta_{\nu} \beta_{\nu+2} \right) = J \cdot m,$$

whereas  $\langle \Phi_{i+\hat{x}+\hat{y}} | H_{\perp} | \Phi_i \rangle = 2J \cdot m$  because a string to a  $(1, 1)$ -like neighbor can pass either through  $(1, 0)$  or  $(0, 1)$  and the contributions from these two different paths are additive.

When the full Hamiltonian  $H_0 + H_{\perp}$  is taken into account the hole therefore can propagate through the entire lattice and we describe this by the Bloch state

$$|\Phi_{\mathbf{k}}\rangle = \sqrt{\frac{2}{N}} \sum_{j \in A} e^{-i\mathbf{k} \cdot \mathbf{R}_j} |\Phi_i\rangle. \quad (22)$$

This is reminiscent of an LCAO wave function such as (1), but the role of the atomic orbital  $|\phi_i\rangle$  here is played by the self-trapped function  $|\Phi_i\rangle$ . Since the matrix element of  $H_{\perp}$  between  $(1, 1)$ -like neighbors is twice that between  $(2, 0)$ -like neighbors we obtain the dispersion

$$\begin{aligned} E_{\mathbf{k}} &= E_{loc} + 2Jm \cdot 4 \cos(k_x) \cos(k_y) + Jm \cdot 2(\cos(2k_x) + \cos(2k_y)) \\ &= E_{loc} - 4Jm + 4Jm(\cos(k_x) + \cos(k_y))^2 \end{aligned} \quad (23)$$

This expression shows several remarkable features which reflect the unusual nature of hole motion. First, there is the constant term  $E_{loc} \propto t$ . As we have seen, in the absence of the spin-flip term  $H_{\perp}$  the hole is self-trapped in a linearly ascending ‘effective potential’ due to magnetic frustration. The hole executes a rapid zig-zag motion on a timescale  $\tau_{loc} \propto t^{-1}$ , and  $E_{loc}$  is the gain of kinetic energy due to this zig-zag motion. Figure 8 shows that  $E_{loc} \approx -2.4 t$  at  $J/t = 0.4$ , which is an appreciable fraction of  $-4t$ , the lowest possible kinetic energy which a freely propagating electron can have in an empty  $2D$  lattice. On the longer time scale  $\tau_{deloc} \propto J^{-1}$ , the

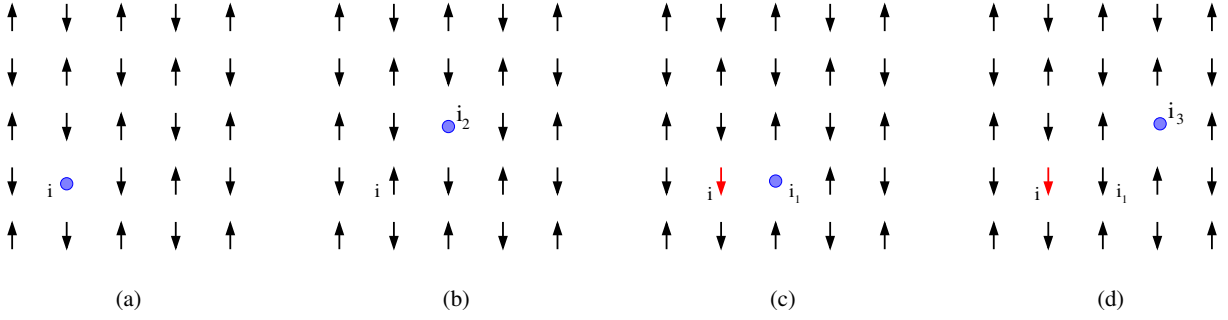


**Fig. 9:** Hopping processes involving a term  $\propto t'$  that connects  $(1, 1)$ -like neighbors.

spin-flip term shifts the center of the zig-zag motion to a  $2^{\text{nd}}$  or  $3^{\text{rd}}$  nearest neighbor, and the zig-zag motion starts anew. It follows that the bandwidth for coherent motion is *not* proportional to the hopping integral  $t$ , but to the smaller exchange constant  $J$ . The total bandwidth is  $16Jm$  and since  $m$  is around 0.14 for  $J/t = 0.4$ , see Figure 8, the bandwidth is roughly  $2J$ . With  $J = 140$  meV as appropriate for cuprates we expect  $W \approx 300$  meV, almost a factor of 10 smaller than the width of the free tight-binding dispersion, which is  $8t \approx 2.8$  eV.  $E_{\mathbf{k}}$  has a degenerate minimum along  $(\pi, 0) \rightarrow (0, \pi)$  and symmetry equivalent lines, its maxima are at  $(0, 0)$  and  $(\pi, \pi)$ . It has ‘antiferromagnetic symmetry’,  $E_{\mathbf{k}+\mathbf{Q}} = E_{\mathbf{k}}$ , which is to be expected since we are considering hole motion in an antiferromagnetic background.

In order to compare our theory to experiment we need to take into account that in the actual  $\text{CuO}_2$ -planes there are appreciable additional hopping integrals  $t'$  between  $(1, 1)$ -like and  $t''$  between  $(2, 0)$ -like neighbors. Since these terms connect pairs of neighbors which are on the same sublattice, they do not create frustration and it might seem that they immediately dominate the hole motion. However, this is not the case and the reason can be seen in Figure 9. Fig. 9(a) shows a ‘string of length 0’, that means a hole at site  $i$  and the hopping term  $\propto t'$  can transport the hole to the  $(1, 1)$ -like neighbor  $i_2$  without creating a magnon. On the other hand, 9(c) shows a ‘string of length 1’, that means a hole which has executed one nearest neighbor hopping process and is now at site  $i_1$ , with a single magnon at site  $i$ . Again, the  $t'$ -term can transport the hole to the  $(1, 1)$ -like neighbor  $i_3$ , but it cannot transport the magnon along with the hole. Therefore, the hopping terms  $\propto t', t''$  can transport only the ‘bare hole’, and since this has the coefficient  $\alpha_0$  in the self-trapped states  $|\Phi_i\rangle$ , these terms are renormalized by a factor  $\alpha_0^2$ . Accordingly, they give the following contribution to the hole dispersion relation

$$E_{tr}(\mathbf{k}) = 4t'\alpha_0^2 \cos(k_x) \cos(k_y) + 2t''\alpha_0^2 (\cos(2k_x) + \cos(2k_y))$$

which has to be added to (23). Note again the opposite sign of the hopping terms as compared to the original Hamiltonian (16) because the fermion operators have to be exchanged to transport a hole. Figure 10 shows a comparison of the modified hole dispersion and the experimental band structure obtained by Angle Resolved Photoemission Spectroscopy (ARPES) on the insulating  $\text{CuO}$ -compound  $\text{Sr}_2\text{CuO}_2\text{Cl}_2$  [11]. The band structure for a hole has to be turned upside down to compare to ARPES because the minimum of the hole-bandstructure is the maximum of the electron-band structure. The agreement is reasonable whereby it has to be kept in mind that in a

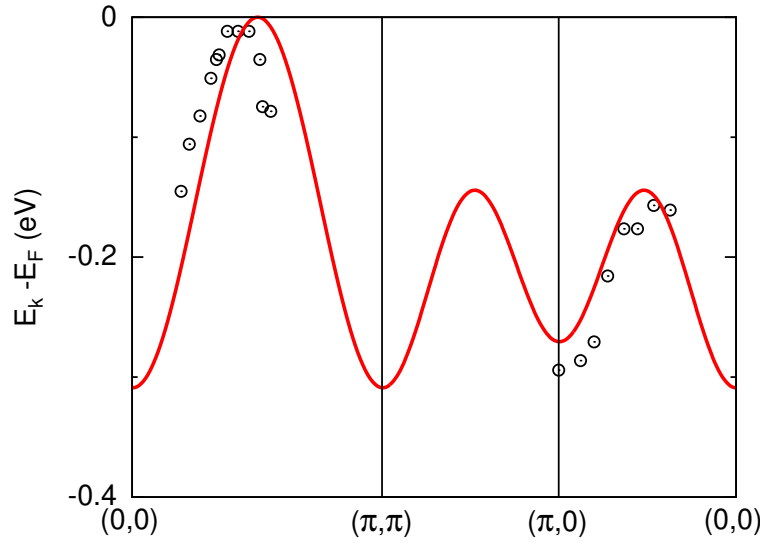


**Fig. 10:** The band structure for the  $t$ - $J$  model with additional hopping terms compared to the experimental valence band structure for the antiferromagnetic insulator  $\text{Sr}_2\text{CuO}_2\text{Cl}_2$  [11]. Parameter values are  $t = 350 \text{ meV}$ ,  $J = 140 \text{ meV}$ ,  $t' = -120 \text{ meV}$ ,  $t'' = 60 \text{ meV}$ .

wide area around  $(\pi, \pi)$  and also close to  $(0, 0)$  the band structure cannot be observed because the band has vanishing spectral weight in ARPES. In any way, the drastic reduction of the bandwidth can be seen clearly.

Looking back, the above discussion illustrates the general remarks in the introduction. In a Mott insulator each site carries a spin and spins on neighboring sites  $i$  and  $j$  are coupled by the exchange term  $J\mathbf{S}_i \cdot \mathbf{S}_j$ . This leads to a tendency for neighboring spins to be antiparallel and the appearance of *spin excitations*, which in the antiferromagnetic phase discussed above take the form of spin waves. Doped holes then have to move through this ‘spin background’ and by their very motion constantly interact with the spin excitations. As we have seen this leads to a drastic modification of the hole motion and band structure. And in fact, this also goes the other way round: since the holes are constantly ‘stirring’ the spins, these react and change their arrangement so as to make hole motion easier and allow for a gain of kinetic energy. In fact, in cuprate superconductors the antiferromagnetic order which was the basis of the above theory breaks down for hole concentrations of only a few per cent. Even in the resulting disordered state, the spin exchange term in the  $t$ - $J$  Hamiltonian still favors antiparallel orientation of spins on nearest neighbors and in fact neutron scattering experiments show that there is still *short range antiferromagnetic order*, i.e., the spin correlation function  $\langle \mathbf{S}_i \cdot \mathbf{S}_{i+\mathbf{R}} \rangle \propto e^{i\mathbf{Q} \cdot \mathbf{R}} e^{-|\mathbf{R}|/\xi}$ . This is reminiscent of the density correlation function in a molten crystal, where locally the correlations between atoms resemble that of the original solid but there is no more long range crystalline order. Accordingly, such a state is called a ‘spin liquid’ and the description of such a spin liquid is the hardest part of the description of the doped Mott-insulator. The main difficulty is that so far nobody has been able to give a wave function for a Heisenberg antiferromagnet that has one electron/site and has no order of any kind. It will become clear in the next paragraph that this requires very drastic and questionable approximations.

## 4 Spin liquids

### 4.1 Dimer basis

As a prelude we follow Sachdev and Bhatt [12] as well as Gopalan, Rice, and Sigrist [13] and consider a *dimer* of two sites, labeled 1 and 2, and assume that both of them are occupied by one electron each, with their spins coupled by the exchange term  $H = J \mathbf{S}_1 \cdot \mathbf{S}_2$ . According to the rules for addition of angular momenta, the two spins of  $1/2$  can be coupled to the total spin  $S = 1$  (spin triplet) or  $S = 0$  (spin singlet). The singlet and the three components of the triplet are eigenstates of the square of the operator of total spin  $\mathbf{S} = \mathbf{S}_1 + \mathbf{S}_2$  with eigenvalue  $S(S+1)$ :  $\mathbf{S}^2 = \mathbf{S}_1^2 + 2\mathbf{S}_1 \cdot \mathbf{S}_2 + \mathbf{S}_2^2 = S(S+1)$ , and using that  $\mathbf{S}_1^2 = \mathbf{S}_2^2 = \frac{1}{2}(\frac{1}{2} + 1) = \frac{3}{4}$  we find  $\mathbf{S}_1 \cdot \mathbf{S}_2 = \frac{1}{2}(S(S+1) - \frac{3}{2})$ . Accordingly,  $\mathbf{S}_1 \cdot \mathbf{S}_2$  gives  $-3/4$  when acting on the singlet and  $1/4$  for a triplet. Due to the limited size of the Hilbert space of the dimer, constructing states with definite total spin thus is equivalent to diagonalizing the exchange term, and we find the eigenenergies  $-3J/4$  for the singlet, and  $J/4$  for the three components of the triplet. The eigenstates themselves are given by [12, 13]

$$\begin{aligned}
 |s\rangle &= \frac{1}{\sqrt{2}} \left( c_{1,\uparrow}^\dagger c_{2,\downarrow}^\dagger - c_{1,\downarrow}^\dagger c_{2,\uparrow}^\dagger \right) |0\rangle, \\
 |t_x\rangle &= \frac{1}{\sqrt{2}} \left( c_{1,\downarrow}^\dagger c_{2,\downarrow}^\dagger - c_{1,\uparrow}^\dagger c_{2,\uparrow}^\dagger \right) |0\rangle, \\
 |t_y\rangle &= \frac{i}{\sqrt{2}} \left( c_{1,\uparrow}^\dagger c_{2,\uparrow}^\dagger + c_{1,\downarrow}^\dagger c_{2,\downarrow}^\dagger \right) |0\rangle, \\
 |t_z\rangle &= \frac{1}{\sqrt{2}} \left( c_{1,\uparrow}^\dagger c_{2,\downarrow}^\dagger + c_{1,\downarrow}^\dagger c_{2,\uparrow}^\dagger \right) |0\rangle.
 \end{aligned} \tag{24}$$

with  $|s\rangle$  the singlet and  $|t_x\rangle$ ,  $|t_y\rangle$  and  $|t_z\rangle$  the three components of the triplet. Note that the three  $|t_\alpha\rangle$  in (24) are *not* eigenstates of the total  $z$ -spin, rather they are linear combinations of the states with fixed  $z$ -spin which obey  $S_\alpha |t_\beta\rangle = i\varepsilon_{\alpha\beta\gamma} |t_\gamma\rangle$ , for example

$$\begin{aligned}
 S_x |t_y\rangle &= \frac{1}{2} \sum_{i=1}^2 (S_i^- + S_i^+) \frac{i}{\sqrt{2}} \left( c_{1,\uparrow}^\dagger c_{2,\uparrow}^\dagger + c_{1,\downarrow}^\dagger c_{2,\downarrow}^\dagger \right) \\
 &= \frac{i}{2\sqrt{2}} \left( c_{1,\downarrow}^\dagger c_{2,\uparrow}^\dagger + c_{1,\uparrow}^\dagger c_{2,\downarrow}^\dagger + c_{1,\uparrow}^\dagger c_{2,\downarrow}^\dagger + c_{1,\downarrow}^\dagger c_{2,\uparrow}^\dagger \right) = i |t_z\rangle.
 \end{aligned}$$

This means that the three states  $|t_\alpha\rangle$  transform like a vector under spin rotations which will be convenient later on. We also note that under the exchange of the two sites,  $1 \leftrightarrow 2$ , we have  $|s\rangle \rightarrow |s\rangle$  but  $|t_\alpha\rangle \rightarrow -|t_\alpha\rangle$ .

We return to the undoped Heisenberg antiferromagnet on a 2D square lattice with  $N$  sites. A state which on the one hand is disordered and on the other hand is an exact spin singlet can be obtained in the following way: let the  $N$  sites be partitioned into  $N/2$  dimers, whereby each dimer comprises two nearest neighbor sites, see Figure 11(a), and assume moreover that the two spins in each dimer are coupled to the singlet state. The resulting state of the plane is the

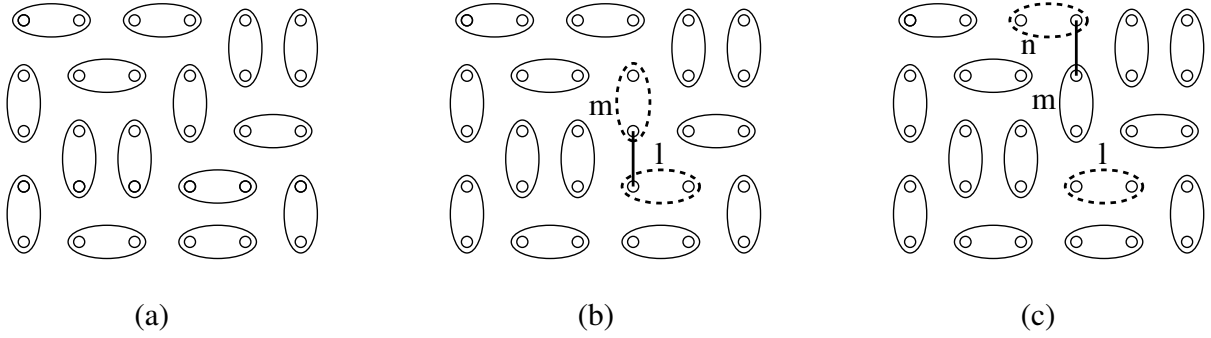


**Fig. 11:** (a) A dimer covering of the plane: spins on sites covered by an ellipse are coupled to a singlet. (b) By acting with the exchange along the bond connecting the dimers  $l$  and  $m$  both dimers are excited into the triplet state. (c) By acting with the exchange along the bond connecting the dimers  $m$  and  $n$  bond  $m$  is de-excited to the singlet whereas dimer  $n$  is excited to the triplet — the triplet has propagated.

product

$$|\Psi_0\rangle = \prod_{(i,j) \in D} \frac{1}{\sqrt{2}} \left( c_{i,\uparrow}^\dagger c_{j,\downarrow}^\dagger - c_{i,\downarrow}^\dagger c_{j,\uparrow}^\dagger \right) |0\rangle$$

where  $D$  is the set of  $N/2$  pairs  $(i, j)$  of nearest neighbor sites corresponding to the given dimer covering.  $|\Psi_0\rangle$  is an eigenstate of the ‘depleted Hamiltonian’  $H_d = J \sum_{(i,j) \in D} \mathbf{S}_i \cdot \mathbf{S}_j$  with eigenvalue  $E_{d,0} = (N/2) \cdot (-3J/4)$ . Since  $\langle \mathbf{S}_i \cdot \mathbf{S}_j \rangle = 0$  if  $i$  and  $j$  belong to different dimers, as will be shown in a moment, this is also the expectation value of the full Hamiltonian in the state  $|\Psi_0\rangle$ . Next, let us consider what happens if we act onto  $|\Psi_0\rangle$  with the exchange along a bond *not* included in the set  $D$ , that means a bond which connects spins in different dimers, such as the bond indicated in Figure 11(b). Due to the product nature of  $|\Psi_0\rangle$  it is sufficient to discuss what happens when the spin operator acts on a singlet, e.g.

$$S_{1,x}|s\rangle = \frac{1}{2}(S_1^- + S_1^+) \frac{1}{\sqrt{2}} \left( c_{1,\uparrow}^\dagger c_{2,\downarrow}^\dagger - c_{1,\downarrow}^\dagger c_{2,\uparrow}^\dagger \right) |0\rangle = \frac{1}{2\sqrt{2}} \left( c_{1,\downarrow}^\dagger c_{2,\downarrow}^\dagger - c_{1,\uparrow}^\dagger c_{2,\uparrow}^\dagger \right) |0\rangle. \quad (25)$$

Comparing with (24), the expression on the right hand side is seen to be  $\frac{1}{2}|t_x\rangle$ . Next, we exchange  $1 \leftrightarrow 2$  on both sides of (25), whence  $S_{1,x} \rightarrow S_{2,x}$ ,  $|s\rangle \rightarrow |s\rangle$ , and  $|t_x\rangle \rightarrow -|t_x\rangle$ , and obtain  $S_{2,x}|s\rangle = -\frac{1}{2}|t_x\rangle$ . Since the triplets were constructed to transform like a vector, this holds true for the other Cartesian components as well:  $S_{1,\alpha}|s\rangle = \frac{1}{2}|t_\alpha\rangle$ ,  $S_{2,\alpha}|s\rangle = \frac{1}{2}|t_\alpha\rangle$  with  $\alpha \in \{x, y, z\}$ . Acting with the term  $J\mathbf{S}_i \cdot \mathbf{S}_j$  along a bond which connects sites  $i$  and  $j$  in different dimers therefore simultaneously excites both dimers to the triplet state, with a prefactor of  $\pm J/4$  (the prefactor will be discussed more precisely below). The new state again is an eigenstate of the ‘depleted Hamiltonian’  $H_d$ , with eigenvalue  $E_{d,0} + 2J$  and obviously is orthogonal to  $|\Psi_0\rangle$ , which also proves that the expectation value  $\langle \mathbf{S}_i \cdot \mathbf{S}_j \rangle$  vanishes if the sites  $i$  and  $j$  belong to different dimers. Next consider what happens when the exchange term acts along the bond indicated in Figure 11(c). We already know that bond  $n$  will be excited to the triplet state but we need to study what happens when the spin operator acts on the triplet in bond

$m$ :

$$S_{1,x}|t_x\rangle = \frac{1}{2}(S_1^+ + S_1^-) \frac{1}{\sqrt{2}} \left( c_{1,\downarrow}^\dagger c_{2,\downarrow}^\dagger - c_{1,\uparrow}^\dagger c_{2,\uparrow}^\dagger \right) |0\rangle = \frac{1}{2\sqrt{2}} \left( c_{1,\uparrow}^\dagger c_{2,\downarrow}^\dagger - c_{1,\downarrow}^\dagger c_{2,\uparrow}^\dagger \right) |0\rangle, \quad (26)$$

which is nothing but  $\frac{1}{2}|s\rangle$ . Therefore, acting with the exchange term along the bond indicated in Figure 11(c), the dimer  $m$  is de-excited to the singlet state according to (26), whereas the dimer  $n$  is excited to the triplet state according to (25) or, put another way, the ‘excited dimer’ jumps from dimer  $m$  to dimer  $n$ . Comparing now with Figure 4 we see a quite analogous pattern arising: both, the Néel state and the dimer state  $|\Psi_0\rangle$  are the ground state of a part of the Hamiltonian, namely the longitudinal part  $J \sum_{\langle i,j \rangle} S_{i,z} S_{j,z}$  in the case of the Néel state and the depleted Hamiltonian  $H_d$  for the dimer state. Switching on the remainder of the Hamiltonian then creates ‘fluctuations’: these were the inverted spins or magnons in the case of the Néel state, and the excited dimers in the case of the singlet soup. The fluctuations increase the energy: by  $zJ/2$  for a magnon, and by  $J$  for a triplet. After having been created these fluctuations then propagate through the lattice. This suggests that we proceed exactly as in the case of spin wave theory and interpret the triplets as effective bosonic particles (we use bosons because a triplet is composed of two electrons). To be more quantitative, we need to introduce some conventions: We assume that the bonds are labeled by a number  $n \in \{1, \dots, N/2\}$ . Since the triplet has negative parity under the exchange of sites,  $1 \leftrightarrow 2$ , we need to specify which of the sites  $i$  and  $j$  in a given dimer corresponds to the site 1 in Eq. (24) and which one to the site 2. We adopt the convention that for a bond in  $x$ -direction ( $y$ -direction) the left (lower) site always corresponds to the site 1. We call the site which corresponds to 1 the ‘1-site of the dimer’ and the site which corresponds to 2 the ‘2-site of the dimer’. For each site  $i$  we define  $\lambda_i = 1$  if it is the 1-site of its respective dimer, and  $-1$  if it is the 2-site. Then, if a given dimer  $m$  is occupied by a singlet, we consider it as occupied by a bosonic particle, created by  $s_m^\dagger$ , whereas if the dimer is in one of the three triplet states we consider it as occupied by a boson, created by  $t_{m,\alpha}^\dagger$  with  $\alpha \in \{x, y, z\}$ . We have already seen that the three triplet states transform like a vector under spin rotations and it follows that the corresponding creation operators form a *vector operator*  $[S_\alpha, t_\beta^\dagger] = i\varepsilon_{\alpha\beta\gamma} t_\gamma^\dagger$ , and Hermitean conjugation shows that the annihilation operator  $t_m$  is a vector operator as well. Calculating the action of the spin operator on triplet states gives the representation of the spin operator

$$\mathbf{S}_j \rightarrow \frac{\lambda_j}{2} (s^\dagger \mathbf{t} + \mathbf{t}^\dagger s) - \frac{i}{2} \mathbf{t}^\dagger \times \mathbf{t}. \quad (27)$$

The  $x$ -component of the correspondence  $\mathbf{S}_j \rightarrow \frac{\lambda_j}{2} (s^\dagger \mathbf{t} + \mathbf{t}^\dagger s)$  was demonstrated in (25) and (26). We recall that we found  $S_{1,x}|s\rangle = \frac{1}{2}|t_x\rangle$  whereas  $S_{2,x}|s\rangle = -\frac{1}{2}|t_x\rangle$  and the factor of  $\lambda_i$  keeps track of this sign. From the discussion after (25) we see that such a sign, and hence a factor of  $\lambda_i$ , will occur whenever the Hamiltonian induces a transition between states which have opposite parity under  $1 \leftrightarrow 2$ . Next, The overall form of the terms on the right hand side follows from the fact that  $\mathbf{S}$  is a Hermitean vector operator, so the right hand side has to be one as well. Then, the vector product  $\mathbf{t}^\dagger \times \mathbf{t}$  is the only way to contract two vector operators into a single one, but since the vector product is anti-Hermitean it has to be multiplied by the factor of  $i$  to make it Hermitean. Next, by forming the scalar product, we can write down the exchange

term  $h_{m,n} = J \mathbf{S}_i \cdot \mathbf{S}_j$  along a bond connecting the sites  $i$  and  $j$  such that site  $i$  belongs to dimer  $m$ , site  $j$  to dimer  $n$  with  $m \neq n$ :

$$\begin{aligned}
h_{m,n} = & \frac{J\lambda_i\lambda_j}{4} \left( \mathbf{t}_n^\dagger \cdot \mathbf{t}_m s_n s_m^\dagger + \mathbf{t}_m^\dagger \cdot \mathbf{t}_n s_m s_n^\dagger + \mathbf{t}_m^\dagger \cdot \mathbf{t}_n^\dagger s_n s_m + \mathbf{t}_m \cdot \mathbf{t}_n s_m^\dagger s_n^\dagger \right) \\
& - \frac{iJ}{4} \left( \lambda_i (s_m^\dagger \mathbf{t}_m + \mathbf{t}_m^\dagger s_m) \cdot (\mathbf{t}_n^\dagger \times \mathbf{t}_n) + \lambda_j (s_n^\dagger \mathbf{t}_n + \mathbf{t}_n^\dagger s_n) \cdot (\mathbf{t}_m^\dagger \times \mathbf{t}_m) \right) \\
& - \frac{J}{4} (\mathbf{t}_n^\dagger \times \mathbf{t}_n) \cdot (\mathbf{t}_m^\dagger \times \mathbf{t}_m). \tag{28}
\end{aligned}$$

As expected the right hand side comprises all possible ways to construct a spin scalar from the vectors  $\mathbf{t}$  and  $\mathbf{t}^\dagger$  and only the numerical prefactors needed to be determined.

## 4.2 Spin excitations

While the representation of the Heisenberg antiferromagnet derived in the preceding section is exact for any given dimer covering of the plane, we have not gained very much because even writing down a dimer covering for a macroscopic system is not feasible, let alone solve the corresponding Hamiltonian. One might consider choosing a particularly ‘simple’ dimer covering such as columns of dimers in, say,  $x$ -direction. However, since one is forced to make approximations, the special symmetry of the covering will make itself felt in the approximate solutions as an artificial supercell structure, leading to a reduction of the Brillouin zone and an unphysical backfolding of bands.

On the other hand, rewriting the Heisenberg Hamiltonian in terms of the singlet and triplet bosons provides an exact representation of the Heisenberg model for *any* dimer covering of the plane. This means that for example the result for the spin correlation function  $\langle \mathbf{S}_j(t) \cdot \mathbf{S}_i \rangle$  cannot depend on the specific dimer covering in which the calculation is carried out. Put another way, the way in which a spin excitation propagates through the network of dimers from site  $i \rightarrow j$  during the time  $t$  does not depend at all on the geometry of the particular dimer covering. This suggests to construct a translationally invariant approximate Hamiltonian by *averaging* the dimer Hamiltonian over all possible coverings. We find

$$H_{av} = J \sum_m \mathbf{t}_m^\dagger \cdot \mathbf{t}_m + \sum_{m,n} \sum_{\substack{i \in m \\ j \in n}} \zeta_{m,n} h_{m,n}. \tag{29}$$

Here we have chosen the energy of the state where all bonds are occupied by triplets as the zero of energy, the first term then adds an energy of  $J$  for every bond occupied by a triplet. The sum  $\sum_{m,n}$  runs over all pairs of bonds connected by an exchange term  $J \mathbf{S}_i \cdot \mathbf{S}_j$  with  $i \in m$  and  $j \in n$  and  $h_{m,n}$  is given in (28). The renormalization factor  $\zeta_{m,n}$  is defined as

$$\zeta_{m,n} = \frac{N_{m,n}}{N_d}, \tag{30}$$

where  $N_{m,n}$  is the number of dimer coverings which contain the bonds  $n$  and  $m$  whereas  $N_d$  is the total number of dimer coverings. The resulting Hamiltonian is translationally invariant and

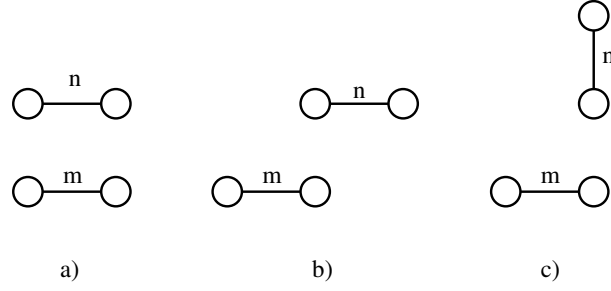


**Fig. 12:** Estimation of the renormalization factor  $\zeta$ .

isotropic. We estimate  $\zeta$  by a crude approximation: consider two adjacent bonds as in Figure 12. By symmetry the bond  $m$  is covered by a dimer in exactly  $1/4$  of all dimer coverings and we restrict ourselves to these. Assuming for simplicity that the number of coverings containing one of the three possible orientations of the adjacent bond  $n$  are equal, we estimate  $\zeta = 1/12$ .

Using the averaging procedure we have circumvented the problem of having to consider a fixed dimer covering, but inspection of (28) shows that  $h_{m,n}$  still is a sum of quartic terms and thus impossible to solve. In the next step of approximation therefore assume that the singlet bosons are condensed and replace the corresponding operators  $s_n^\dagger$  and  $s_n$  in (28) by the real *condensation amplitude*  $s$ . This is equivalent to assuming that the singlets form an inert background and the only active degrees of freedom are the triplets. Further inspection of (28) shows that after singlet condensation it contains terms of second, third and fourth order in the triplet operators. As the final approximation we discard the terms of third and fourth order, which describe scattering processes between the triplets, whence the Hamiltonian finally becomes

$$H_{av} = \tilde{J} \sum_m \mathbf{t}_m^\dagger \cdot \mathbf{t}_m + \frac{\zeta s^2}{4} \sum_{m,n} \sum_{\substack{i \in m \\ j \in n}} J_{i,j} \lambda_i \lambda_j (\mathbf{t}_n^\dagger \cdot \mathbf{t}_m + \mathbf{t}_m^\dagger \cdot \mathbf{t}_n + \mathbf{t}_m^\dagger \cdot \mathbf{t}_n^\dagger + \mathbf{t}_n \cdot \mathbf{t}_m). \quad (31)$$

The sums over  $m, n$  run over all  $2N$  bonds of the plane,  $J_{i,j} = J$  if  $i$  and  $j$  are nearest neighbors and zero otherwise.

From this point on we can proceed exactly in the same way as we did for the antiferromagnetic magnons. Being a quadratic form (31) is readily diagonalized by Fourier transform, we only need to specify a convention for the position of a bond: if bond  $m$  connects the sites  $i$  and  $j$  we define  $\mathbf{R}_m = (\mathbf{R}_i + \mathbf{R}_j)/2$ . Moreover we have two species of bonds: bonds in  $x$ -directions and bonds in  $y$ -direction. We specify this by an additional subscript for the Fourier transformed operators, e.g.  $\mathbf{t}_{\mathbf{k},\mu}^\dagger$  with  $\mu \in \{x, y\}$ . The products  $\lambda_i \lambda_j$  are given in Figure 13 from which we readily can read off

$$H = \sum_{\mathbf{k}} \sum_{\mu, \mu' \in \{x, y\}} \left( \mathbf{t}_{\mathbf{k},\mu}^\dagger (\tilde{J} \delta_{\mu\mu'} + \varepsilon_{\mu,\mu'}(\mathbf{k})) \mathbf{t}_{\mathbf{k},\mu'} + \frac{1}{2} (\mathbf{t}_{\mathbf{k},\mu}^\dagger \varepsilon_{\mu,\mu'}(\mathbf{k}) \mathbf{t}_{-\mathbf{k},\mu'}^\dagger + H.c.) \right)$$

$$\varepsilon_{x,x}(\mathbf{k}) = \zeta s^2 J \left( \cos(k_y) - \frac{1}{2} \cos(2k_x) - \cos(k_x) \cos(k_y) \right),$$

$$\varepsilon_{x,y}(\mathbf{k}) = \zeta s^2 J \left( \sin\left(\frac{3k_x}{2}\right) \sin\left(\frac{k_y}{2}\right) + \sin\left(\frac{k_x}{2}\right) \sin\left(\frac{3k_y}{2}\right) \right),$$

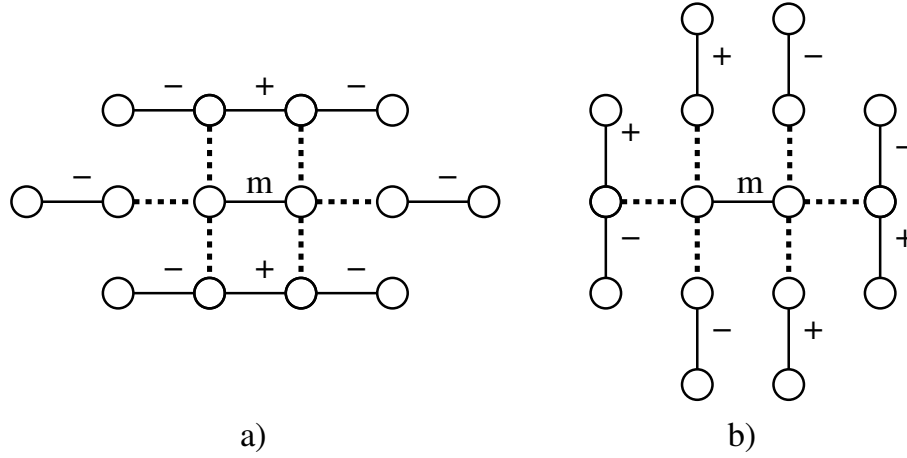


**Fig. 13:** The factors of  $\lambda_i \lambda_j$  for all bonds connected to the bond  $m$  by a nearest neighbor bond. In a) both bonds are along the  $x$ -direction so that these pairs contribute to  $\varepsilon_{x,x}$  whereas in b) one bond is along the  $y$ -direction so that these pairs contribute to  $\varepsilon_{x,y}$ . In a) both bonds connecting parallel bonds have  $\lambda_i \lambda_j = 1$ .

$\varepsilon_{y,x} = \varepsilon_{x,y}$ , and  $\varepsilon_{y,y}$  is obtained from  $\varepsilon_{x,x}$  by  $k_x \leftrightarrow k_y$ . To diagonalize  $H$  we proceed as for antiferromagnetic magnons and make the *ansatz* (with  $\nu \in \{1, 2\}$ )

$$\begin{aligned}\tau_{\nu,\mathbf{k}}^\dagger &= \sum_{\mu \in \{x,y\}} (u_{\nu,\mathbf{k},\mu} \mathbf{t}_{\mathbf{k},\mu}^\dagger + v_{\nu,\mathbf{k},\mu} \mathbf{t}_{-\mathbf{k},\mu}), \\ \tau_{\nu,-\mathbf{k}} &= \sum_{\mu \in \{x,y\}} (v_{\nu,\mathbf{k},\mu}^* \mathbf{t}_{\mathbf{k},\mu}^\dagger + u_{\nu,\mathbf{k},\mu}^* \mathbf{t}_{-\mathbf{k},\mu}).\end{aligned}\quad (32)$$

Demanding  $[H, \tau_{\nu,\mathbf{k}}^\dagger] = \omega_{\nu,\mathbf{k}} \tau_{\nu,\mathbf{k}}^\dagger$  gives the  $4 \times 4$  eigenvalue problem

$$\begin{pmatrix} \tilde{J} + \varepsilon_{\mathbf{k}} & -\varepsilon_{\mathbf{k}} \\ \varepsilon_{-\mathbf{k}}^* & -\tilde{J} - \varepsilon_{-\mathbf{k}}^* \end{pmatrix} \begin{pmatrix} u_{\nu,\mathbf{k}} \\ v_{\nu,\mathbf{k}} \end{pmatrix} = \omega_{\nu,\mathbf{k}} \begin{pmatrix} u_{\nu,\mathbf{k}} \\ v_{\nu,\mathbf{k}} \end{pmatrix}.\quad (33)$$

For a matrix like the one on the left hand side it is easy to show that if  $(u, v)$  is an eigenvector with eigenvalue  $\omega$ , then  $(v^*, u^*)$  is an eigenvector with eigenvalue  $-\omega$  so that the eigenvalues come in pairs of  $\pm\omega$ . We multiply (33) by  $\omega_{\nu,\mathbf{k}}$  and replace products such as  $\omega_{\nu,\mathbf{k}} u_{\nu,\mathbf{k}}$  or  $\omega_{\nu,\mathbf{k}} v_{\nu,\mathbf{k}}$  on the left hand side of the resulting equations by the expressions given by the original version of (33). Since the commutator  $[\tilde{J} + \varepsilon_{\mathbf{k}}, \varepsilon_{\mathbf{k}}] = 0$  we obtain

$$(\tilde{J}^2 + 2\tilde{J}\varepsilon_{\mathbf{k}})u_{\nu,\mathbf{k}} = \omega_{\nu,\mathbf{k}}^2 u_{\nu,\mathbf{k}},$$

and the same equation for  $v_{\nu,\mathbf{k}}$ . It follows that  $\omega_{\nu,\mathbf{k}} = \sqrt{\tilde{J}^2 + 2\tilde{J}\lambda_{\nu,\mathbf{k}}}$ , where  $\lambda_{\nu,\mathbf{k}}$  are the eigenvalues of the Hermitean  $2 \times 2$  matrix  $\varepsilon_{\mathbf{k}}$ , and both,  $u_{\nu,\mathbf{k}}$  and  $v_{\nu,\mathbf{k}}$ , must be the corresponding eigenvector, albeit multiplied by different prefactors. The eigenvalues of  $\varepsilon_{\mathbf{k}}$  are easily shown to be  $\lambda_{1,\mathbf{k}} = -\zeta s^2 J/2$  and  $\lambda_{2,\mathbf{k}} = \zeta s^2 J(3/2 + 2\gamma_{\mathbf{k}} - 4\gamma_{\mathbf{k}}^2)$ , with  $\gamma_{\mathbf{k}}$  given in (12).

In principle the singlet condensation amplitude  $s$  and the renormalized triplet energy  $\tilde{J}$  should now be calculated self-consistently, but for the sake of simplicity we here switch to a more

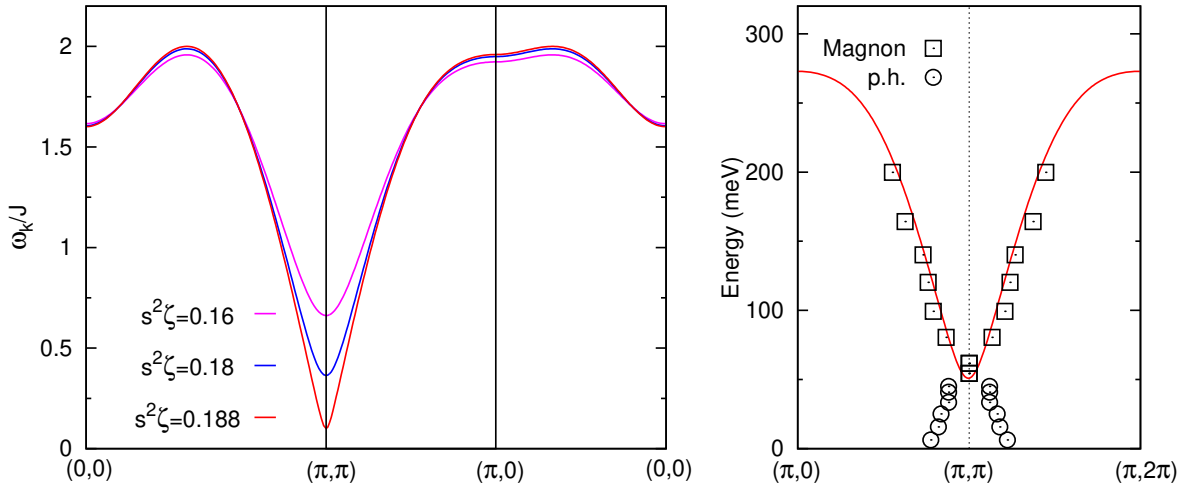


**Fig. 14:** Left: Spin excitation dispersion relation  $\omega_{\mathbf{k}}$  using the parameter values  $\tilde{J} = 1.7 J$  and different  $s^2\zeta$ . Right:  $\omega_{\mathbf{k}}$  calculated for  $\tilde{J} = 1.7 J$ ,  $s^2\zeta = 0.16$  and  $J = 140$  meV compared to the hourglass dispersion measured in  $\text{La}_{1.875}\text{Ba}_{0.125}\text{CuO}_4$  [14]. The data points labeled ‘Magnon’ correspond to the triplet dispersion, the points labeled ‘p.h.’ correspond to particle-hole excitations which are absent in our theory.

phenomenological description and consider  $s^2\zeta$  and  $\tilde{J}$  as adjustable parameters. Regarding  $s^2\zeta$  we recall that  $\zeta$  was determined somewhat vaguely anyway. Regarding  $\tilde{J}$  we expect  $\tilde{J} > J$  because  $\tilde{J}$  gives the cost in energy needed to create a triplet. This is of course  $J$  itself, but should be augmented by a loss of kinetic energy that is incurred because a triplet on, say, dimer  $m$  blocks pair creation and hopping processes on all dimers that share a site with  $m$ . Our theory thus has two adjustable parameters, which we use to fix two physical quantities, the total bandwidth of the spin excitations, and the spin gap (to be explained below). Lastly, we recall that we have two eigenvalues  $\lambda_{\nu,\mathbf{k}}$  for each wave vector  $\mathbf{k}$ , whereby  $\lambda_{1,\mathbf{k}}$  has the peculiar feature of being independent of  $\mathbf{k}$ . A more detailed analysis shows [15], that the band derived from the dispersionless eigenvalue also has zero spectral weight in the spin correlation function. This suggests, that this band is an artifact of the enlargement of the basis by doubling the number of bonds. We therefore drop this dispersionless band and retain only the band of spin excitations resulting from  $\lambda_{2,\mathbf{k}}$ . Figure 14 shows the resulting triplet dispersion  $\omega_{\mathbf{k}}$ . The parameter  $\tilde{J}$  has been adjusted to set the total bandwidth to  $2J$ , the bandwidth for antiferromagnetic spin waves.  $\omega_{\mathbf{k}}$  has a minimum at  $(\pi, \pi)$  and the energy at this wave vector is frequently called the spin gap,  $\Delta_S$ . With increasing value of  $s^2\zeta$ ,  $\Delta_S$  closes rapidly and one can envisage how for  $\Delta_S \rightarrow 0$  the cone-shaped dispersion of antiferromagnetic spin waves at  $(\pi, \pi)$  is recovered. Experimentally, inelastic neutron scattering on many cuprate compounds shows an ‘hourglass’ dispersion around  $(\pi, \pi)$ , an example is also shown in Figure 14. This is frequently interpreted [16] as a magnon-like collective mode above the neck of the hour-glass co-existing with particle-hole excitations of the Fermi gas of free carriers below the neck. The part above the neck of the hourglass thus should correspond to our triplet band and the comparison in Figure 14 shows indeed reasonable agreement.

### 4.3 Doped holes

Next, we extend the theory for the spin liquid to include doped holes. As the first step we introduce dimers which contain a single electron or no electron at all. We again consider a dimer with sites 1 and 2, but now assume that the dimer contains one electron with spin  $\sigma$ . Instead of the exchange term, it is now the hopping term which is active:  $H_t = -t \sum_{\sigma} (\hat{c}_{1,\sigma}^{\dagger} \hat{c}_{2,\sigma} + H.c.)$  and there are two eigenstates of  $H_t$

$$|f_{\pm,\sigma}\rangle = \frac{1}{\sqrt{2}} (\hat{c}_{1,\sigma}^{\dagger} \pm \hat{c}_{2,\sigma}^{\dagger}) |0\rangle. \quad (34)$$

These obey  $H_t |f_{\pm,\sigma}\rangle = \mp t |f_{\pm,\sigma}\rangle$ . We introduce a new type of effective particle to represent dimers occupied by one electron. If the dimer  $m$  is in one of the states  $|f_{\pm,\sigma}\rangle$  we consider it as occupied by a fermion, created by  $f_{m,\pm,\sigma}^{\dagger}$ . We choose a fermion, because the number of electrons in such a dimer is one. We also introduce an additional boson, created by  $e^{\dagger}$ , to represent an empty dimer. In order to include these particles we need to transcribe the electron creation and annihilation operators  $\hat{c}_{i,\sigma}^{\dagger}$  and  $\hat{c}_{i,\sigma}$ . The two spin components of a fermion creation operator can be combined to a two-component vector, a covariant spinor [17],  $\mathbf{c}^{\dagger} = (c_{\uparrow}^{\dagger}, c_{\downarrow}^{\dagger})^T$ . Similarly the spin components of the annihilation operator for a so-called contravariant spinor  $\mathbf{c} = (c_{\uparrow}, c_{\downarrow})^T$ . Proceeding in an analogous way as in the derivation of (27) for the spin operator we find (with  $j \in \{1, 2\}$ )

$$\mathbf{c}_j \rightarrow : \frac{1}{2} (s i\tau_y + \lambda_j \mathbf{t} \cdot \boldsymbol{\tau} i\tau_y) (\mathbf{f}_+^{\dagger} - \lambda_j \mathbf{f}_-^{\dagger}) + \frac{1}{\sqrt{2}} e^{\dagger} (\mathbf{f}_+ + \lambda_j \mathbf{f}_-) : \quad (35)$$

where  $: \dots :$  denotes normal ordering. The first term on the right hand side describes a singlet or triplet state on a given bond being converted into a single-electron state, the second term describes a single-hole state being converted into the empty bond. As was the case for the triplets, the overall form of the terms on the right hand side can be guessed by making use of the transformation properties under spin rotations. The so-called metric spinor  $i\tau_y$  converts the covariant spinors  $\mathbf{f}_{\pm}^{\dagger}$  into contravariant ones [17] and the ‘spinor product’  $\mathbf{t} \cdot \boldsymbol{\tau} \mathbf{c}$  is the only way to construct a contravariant spinor from the vector operator  $\mathbf{t}$  and another contravariant spinor  $\mathbf{c}$ . The factors of  $\lambda_j$  again are associated with states of opposite parity under  $1 \leftrightarrow 2$ . Using (35) we can rewrite the hopping term, along a bond connecting the sites  $i$  and  $j$  such that site  $i$  belongs to dimer  $m$ , site  $j$  to dimer  $n$

$$\begin{aligned} -t \sum_{\sigma} \hat{c}_{i,\sigma}^{\dagger} \hat{c}_{j,\sigma} &\rightarrow \frac{t}{4} \left( (s_m^{\dagger} s_n + \lambda_i \lambda_j \mathbf{t}_m^{\dagger} \cdot \mathbf{t}_n) \left( \sum_{\sigma} f_{n,j,\sigma}^{\dagger} f_{m,i,\sigma} \right) \right. \\ &\quad \left. - (\lambda_i \mathbf{t}_m^{\dagger} s_n + \lambda_j s_m^{\dagger} \mathbf{t}_n) \cdot \mathbf{v}_{(n,j),(m,i)} - i \lambda_i \lambda_j (\mathbf{t}_m^{\dagger} \times \mathbf{t}_n) \cdot \mathbf{v}_{(n,j),(m,i)} \right), \end{aligned} \quad (36)$$

where the combination  $f_{m,i,\sigma} = f_{m,+,\sigma} - \lambda_i f_{m,-,\sigma}$  and the vector

$$\mathbf{v}_{(n,j),(m,i)} = \sum_{\sigma,\sigma'} f_{n,j,\sigma}^{\dagger} \boldsymbol{\tau}_{\sigma,\sigma'} f_{m,i,\sigma'}$$

obeys  $[S_{\alpha}, v_{\beta}] = i \varepsilon_{\alpha\beta\gamma} v_{\gamma}$ . Again, the right hand side in (36) is a linear combination of all possible ways to construct a spin scalar from two spinors and zero, one, or two vector operators.

Next, we proceed as in the case of the triplet Hamiltonian. We again average the Hamiltonian over dimer coverings, again introducing the factors of  $\zeta$ , and replace the singlet operators  $s_m^\dagger$ ,  $s_m$  by the real singlet condensation amplitude  $s$ . Lastly we discard all terms which describe the emission/absorption of a triplet by a fermion or the scattering of a fermion from a triplet. With these simplifications we obtain the fermionic Hamiltonian

$$H_F = -t \sum_{m,\sigma} (f_{m,+,\sigma}^\dagger f_{m,+,\sigma} - f_{m,-,\sigma}^\dagger f_{m,-,\sigma}) + \frac{s^2 \zeta}{4} \sum_{m,n} \sum_{\substack{i \in m \\ j \in n}} t_{i,j} \sum_{\sigma} f_{n,j,\sigma}^\dagger f_{m,i,\sigma}, \quad (37)$$

where the sum over  $m, n$  run over all  $2N$  bonds in the system and  $t_{i,j} = t$  if  $i$  and  $j$  are nearest neighbors and zero otherwise.

Next, we switch to the question about how to count electrons. Obviously, each  $f_{m,\pm,\sigma}^\dagger$ -fermion contains one hole and has a  $z$ -spin of  $\sigma$ . Accordingly, in a given dimer covering the number of fermions must be equal to the number of doped holes, which is  $N - N_e$

$$N - N_e = \sum_{m,\sigma} (f_{m,+,\sigma}^\dagger f_{m,+,\sigma} + f_{m,-,\sigma}^\dagger f_{m,-,\sigma}), \quad (38)$$

where the sum over  $m$  runs over the  $N/2$  dimers. We have obtained an approximate theory by averaging over dimer coverings, so that each of the  $2N$  bonds in the plane can be occupied by a boson or fermion. The physically relevant quantity, however, is the *density of holes per site*, whereas the number of dimers loses its significance due to the averaging approximation. Accordingly, we retain the condition (38), but the sum over  $m$  now runs over all  $2N$  bonds in the system. This condition implies, that the bands obtained by diagonalizing (37) have to be filled from below with  $N - N_e = N\delta$  holes, and since the  $f_{m,\pm,\sigma}^\dagger$ -fermions have a spin of  $1/2$  the Fermi surface covers a fraction of  $\delta/2$  of the Brillouin zone. We recall that this is precisely what we found in the framework of the Hubbard-I approximation. This is no surprise if we recall our discussion of spin-charge-separation in the context of the Hubbard-I approximation. There we noted that while a vacancy is a spinless object, the Hubbard-I approximation implicitly assumes that the information about the spin of the missing electron is ‘stored’ in the neighborhood of the vacancy and moves along with the vacancy. This is precisely the case in the dimer theory, where remaining electron in the dimer has opposite spin to the missing electron whence the dimers containing holes in fact are spin- $1/2$  particles.

We continue with the discussion of the band structure. We are interested mainly in the lowermost bands, these are the ones which will accommodate the doped holes, so for simplicity we drop the  $f_{m,-,\sigma}^\dagger$ -fermions, because their energy is  $2t$  above that of the  $f_{m,+,\sigma}^\dagger$ -fermions, whereas the dispersive terms are  $\propto s^2 \zeta t \approx 0.2 t$ . With this last approximation Fourier transformation gives  $H_F = \sum_{\mathbf{k},\sigma} v_{\mathbf{k},\sigma}^\dagger \tilde{H}_{\mathbf{k}} v_{\mathbf{k},\sigma}$  with the vector  $v_{\mathbf{k},\sigma} = (f_{\mathbf{k},x,+,\sigma}, f_{\mathbf{k},y,+,\sigma})^T$ . The  $\mathbf{k}$ -dependence of the  $2 \times 2$  matrix  $\tilde{H}_{\mathbf{k}}$  can again be read off from Figure 13, but with all  $\lambda = 1$ . We obtain

$$\begin{aligned} \tilde{H}_{x,x} &= -t + s^2 \zeta t \left( \cos(k_y) + \cos(k_x) \cos(k_y) + \frac{1}{2} \cos(2k_x) \right) \\ \tilde{H}_{x,y} &= s^2 \zeta t \left( \cos\left(\frac{3k_x}{2}\right) \cos\left(\frac{k_y}{2}\right) + \cos\left(\frac{k_x}{2}\right) \cos\left(\frac{3k_y}{2}\right) \right). \end{aligned}$$

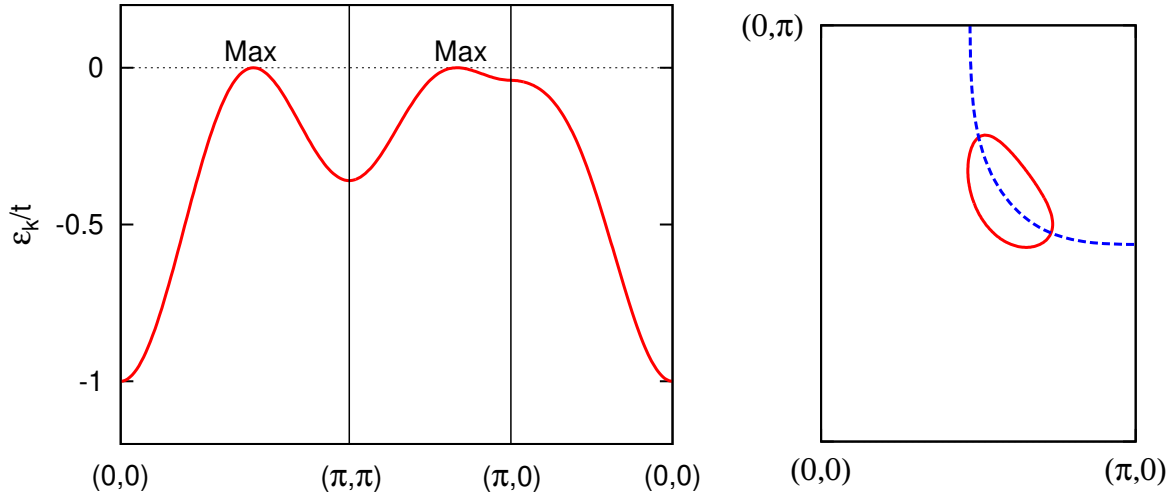


**Fig. 15:** *Left: Dispersion relation  $-\varepsilon_{2,\mathbf{k}}$  for  $s^2\zeta = 0.16$ . Holes would occupy the maxima of this band as indicated in the Figure, so that the zero of energy corresponds roughly to the Fermi energy for small doping. Right: Adding additional hopping terms between  $(1, 1)$  and  $(2, 0)$ -like neighbors lifts the degeneracy of the band maximum (indicated in blue) and the Fermi surface takes the form of a hole pocket (indicated in red) [15]. The values  $t' = -0.2t$ ,  $t'' = 0.1t$  and the hole concentration  $\delta = 1 - n_e = 0.1$ .*

$\tilde{H}_{y,x} = \tilde{H}_{x,y}$  and  $\tilde{H}_{y,y}$  is obtained from  $\tilde{H}_{x,x}$  by  $k_x \leftrightarrow k_y$ . The eigenvalues of  $\tilde{H}_{\mathbf{k}}$  are  $\varepsilon_{1,\mathbf{k}} = -t + s^2\zeta t/2$  and  $\varepsilon_{2,\mathbf{k}} = -t + s^2\zeta t(-3/2 + 2\gamma_{\mathbf{k}} + 4\gamma_{\mathbf{k}}^2)$ . More detailed investigation again shows [15] that the dispersionless band  $\varepsilon_{1,\mathbf{k}}$  has zero weight in the electron spectral function, so again we interpret this as an artifact of the enlargement of the basis states and discard it. As we have seen above the band structure resulting from (37) has to be filled with holes from below, that means at  $T = 0$  the condition for the Fermi energy  $E_F$  is

$$\delta = \frac{2}{N} \sum_{\mathbf{k}} \Theta(\varepsilon_{2,\mathbf{k}} - E_F).$$

Figure 15 shows  $-\varepsilon_{2,\mathbf{k}}$ , that means the band is again turned upside down as it would be seen in ARPES. The maxima therefore correspond to the minima of  $\varepsilon_{2,\mathbf{k}}$ , and this is the location in  $\mathbf{k}$ -space where the doped holes would accumulate.  $\varepsilon_{2,\mathbf{k}}$  depends on  $\mathbf{k}$  only via  $\gamma_{\mathbf{k}}$ , so that lines of constant  $\gamma_{\mathbf{k}}$  automatically are lines of constant  $\varepsilon_{2,\mathbf{k}}$ , in particular the maximum of the inverted dispersion is a roughly circular contour around  $(\pi, \pi)$ . The Fermi surface therefore would be a ring with a width  $\propto \delta$ , which does not agree with ARPES results. However, we recall that in the actual  $\text{CuO}_2$  planes there are the additional hopping terms  $\propto t', t''$  discussed above and inclusion of the terms indeed lifts the degeneracy and leads to a Fermi surface which takes the form of a hole pocket centered along the  $(1, 1)$  direction, see Figure 15. Compared to experiment, the pocket is shifted towards  $(\pi, \pi)$ , but it should be noted that we have made many simplifications and a qualitative agreement with experiment is already a reasonable result.

## 5 Summary and Outlook

As explained in the introduction, the hallmark of a Mott insulator is the breakdown of the Fermi surface due to the effectively enhanced Coulomb repulsion in ‘small’ atomic orbitals: if the number of electrons is equal to the number of sites,  $N$ , the electrons are caught in a ‘traffic jam’ and form a spin system instead of a half-filled band with a Fermi surface. The spins interact via virtual hopping processes of electrons as described by the Heisenberg exchange, which leads to antiferromagnetic correlations and spin excitations.

In the description of the *doped* Mott insulator given in the preceding sections, the electrons continue to form a mere spin system: the majority of electrons are coupled to inert (‘condensed’) singlets, a few singlets are excited to the triplet state, so that most electrons still contribute only their spin degrees of freedom. This is not surprising, because for a low density of vacancies, most electrons still are completely surrounded by other electrons and thus ‘stuck’. Instead, the true mobile fermions in the system are the  $f^\dagger$ -particles, which may be viewed as tightly bound states of a spinless hole and one spin, and their number equals the doped holes. Since the  $f^\dagger$ -particles have a spin of  $1/2$ , their Fermi surface covers a fraction  $\delta/2$  of the Brillouin zone, where  $\delta = 1 - n_e$  is the concentration of *holes*. We recall that for free electrons the fraction of the Brillouin zone covered by the Fermi surface is  $n_e/2$ , which differs drastically from  $\delta/2$ .

On the other hand, we expect that the state where the electrons are ‘jammed’ and form an inert background can persist only over a limited range of the hole concentration  $\delta$ . A crude estimate for the range of stability of this phase can be obtained by noting that once  $\delta$  reaches  $1/z = 0.25$ , on average each electron will find an empty site on one of its  $z$  neighbors to which it can hop without creating a double occupancy. With increasing  $\delta$  it therefore will become energetically favorable for the electrons to form the all-electron Fermi surface of the free electron gas, although the strong scattering will lead to correlation narrowing of the quasiparticle band and strong incoherent weight in the single-particle spectral function. In fact, in the limit  $n_e \rightarrow 0$  it is known [3] that one recovers a Fermi surface with volume  $n_e/2$  but enhanced effective mass. Accordingly, at some critical  $\delta_c$  we expect a phase transition from the doped Mott-insulator with a hole-like Fermi surface of fractional volume  $\delta/2$  described by the above theory, to a renormalized all-electron Fermi liquid with an electron-like Fermi surface of fractional volume  $n_e/2$ . And in fact the experimental situation has pretty much converged to this scenario: a transition between two nonmagnetic Fermi liquids of spin- $1/2$  particles without any obvious order but different Fermi surface volume, which occurs at a hole concentration  $n_{h,c} \approx 0.22$ . This is discussed in detail in Ref. [15]. Assuming that this  $T = 0$  phase transition ‘shrouds itself in superconductivity’ as quantum phase transitions often do, one arrives at the well-known phase diagram of cuprate superconductors. In fact, unlike many other quantum phase transitions, the transition in the cuprates appears to be between two phases which are homogeneous, isotropic and nonmagnetic and differ only in the Fermi surface volume, so that there is no obvious order parameter. This would be consistent with the above scenario. The detailed description of this transition and how it can give rise to the spectacularly high superconducting transition temperatures is probably the key problem in understanding cuprate superconductors.

## References

- [1] J.G. Bednorz and K.A. Müller, *Z. Phys. B* **64**, 189 (1986)
- [2] J. Hubbard, *Proc. Roy. Soc. London A* **276** 238 (1963)
- [3] A.L. Fetter and J.D. Walecka, *Quantum Theory of Many-Particle Systems* (McGraw-Hill, San Francisco, 1971)
- [4] K.A. Chao, J. Spałek, A.M. Oleś, *J. Phys. C* **10**, L 271 (1977)
- [5] P.W. Anderson, *Phys. Rev.* **86**, 694 (1952)
- [6] R. Coldea, S.M. Hayden, G. Aeppli, T.G. Perring, C.D. Frost, T.E. Mason, S.-W. Cheong, and Z. Fisk, *Phys. Rev. Lett.* **86**, 5377 (2001)
- [7] F.C. Zhang, T.M. Rice, *Phys. Rev. B* **37**, 3759 (1988)
- [8] L.N. Bulaevskii, E.L. Nagaev, and D.L. Khomskii, *Sov. Phys. JETP.* **27**, 836 (1968)
- [9] S.A. Trugman, *Phys. Rev. B* **37**, 1597 (1988); *ibid* **41**, 892 (1990)
- [10] R. Eder and K.W. Becker, *Z. Phys. B* **78**, 219 (1990)
- [11] S. LaRosa, I. Vobornik, F. Zwick, H. Berger, M. Grioni, G. Margaritondo, R.J. Kelley, M. Onellion, and A. Chubukov *Phys. Rev. B* **56**, R525 (1997)
- [12] S. Sachdev and R.N. Bhatt, *Phys. Rev. B* **41**, 9323 (1990)
- [13] S. Gopalan, T.M. Rice, and M. Sigrist, *Phys. Rev. B* **49**, 8901 (1994)
- [14] J.M. Tranquada, H. Woo, T.G. Perring, H. Goka, G.D. Gu, G. Xu, M. Fujita, and K. Yamada, *Nature* **429** 534 (2004)
- [15] R. Eder, *Phys. Rev. B* **100**, 085133 (2019)
- [16] M. Fujita, H. Hiraka, M. Matsuda, M. Matsuura, J.M. Tranquada, S. Wakimoto, G. Xu, and K. Yamada, *J. Phys. Soc. Jpn.* **81**, 011007 (2012)
- [17] L.D. Landau and E.M. Lifshitz: *Lehrbuch der Theoretischen Physik* (Akademie Verlag, Berlin, 1988)